

# A Recovery-Based A Posteriori Error Estimator for $\mathbf{H}(\mathbf{curl})$ Interface Problems \*

Zhiqiang Cai <sup>†</sup> Shuhao Cao <sup>‡</sup>

## Abstract

This paper introduces a new recovery-based a posteriori error estimator for the lowest order Nédélec finite element approximation to the  $\mathbf{H}(\mathbf{curl})$  interface problem. The error estimator is analyzed by establishing both the reliability and the efficiency bounds and is supported by numerical results. Under certain assumptions, it is proved that the reliability and efficiency constants are independent of the jumps of the coefficients.

## 1 Introduction

Let  $\Omega \subset \mathbb{R}^3$  be a bounded polyhedral domain with Lipschitz boundary. Let  $\mathcal{P} = \{\Omega_j\}_{j=1}^m$  be a partition of the domain  $\Omega$  with each subdomain  $\Omega_j$  being polyhedron. The collection of interfaces  $(\bigcup_{j=1}^m \partial\Omega_j) \setminus \partial\Omega$  is denoted by  $\mathfrak{I}$ . Assume that  $\mu$  and  $\beta$  are piecewise, positive constants with respect to the partition  $\mathcal{P}$ . We consider the following  $\mathbf{H}(\mathbf{curl})$  interface problem:

$$\begin{cases} \nabla \times (\mu^{-1} \nabla \times \mathbf{u}) + \beta \mathbf{u} = \mathbf{f}, & \text{in } \Omega, \\ \mathbf{u} \times \mathbf{n} = \mathbf{g}, & \text{on } \partial\Omega, \end{cases} \quad (1.1)$$

where  $\mathbf{n}$  is the unit outward vector normal to the boundary of  $\Omega$ . This model problem originates from a stable marching scheme of the second-order hyperbolic partial differential equation on the electric field intensity  $\mathbf{u}$  that is resulted from the Maxwell equations (e.g. see [19, 23]). The  $\mu$  is the magnetic permeability, and the  $\beta \sim \frac{\epsilon}{\Delta t^2} + \frac{\sigma}{\Delta t}$  is related to the dielectric constant  $\epsilon$  and conductivity  $\sigma$  scaled by the time-marching step size  $\Delta t$ . The boundary data  $\mathbf{g}$  is “admissible” in a sense

---

\*This work was supported in part by the National Science Foundation under grant DMS-1217081.

<sup>†</sup>Department of Mathematics, Purdue University, 150 N. University Street, West Lafayette, IN 47907-2067, zcai@math.purdue.edu.

<sup>‡</sup>Department of Mathematics, Pennsylvania State University, University Park, State College, PA 16802, scao@psu.edu.

that we will elaborate when introducing the finite element approximation (2.15). Throughout this article, boldface letters stand for vector fields and spaces of vector fields, non-boldface letters stand for scalar functions and spaces of scalar functions.

The variational formulation of problem (1.1) involves the Hilbert space  $\mathbf{H}(\mathbf{curl})$ , which is the collection of all square integrable vector fields whose curl are also square integrable:

$$\mathbf{H}(\mathbf{curl}; \Omega) := \{\mathbf{v} \in \mathbf{L}^2(\Omega) : \nabla \times \mathbf{v} \in \mathbf{L}^2(\Omega)\}. \quad (1.2)$$

The right hand side data  $\mathbf{f}$  depends on the original source current and on the electric field intensity at previous time steps in the time-marching scheme. In almost all relevant literatures,  $\mathbf{f}$  is assumed to be divergence free. In this paper, we assume that  $\mathbf{f} \in \mathbf{H}(\text{div})$ , where  $\mathbf{H}(\text{div})$  is the analog of the  $\mathbf{H}(\mathbf{curl})$  space for the divergence operator:

$$\mathbf{H}(\text{div}; \Omega) := \{\mathbf{v} \in \mathbf{L}^2(\Omega) : \nabla \cdot \mathbf{v} \in L^2(\Omega)\}. \quad (1.3)$$

For the finite element approximation to (1.1), Nédélec introduced the  $\mathbf{H}(\mathbf{curl})$ -conforming edge elements in [28], which preserves the continuity of the tangential components, and certain *a priori* error estimates can be established (e.g. see [27]). However, the electromagnetic fields have limited regularities at reentrant corners and material interfaces (see [16, 18]). Hence the assumptions for *a priori* error estimates fail, and this is where adaptive mesh refinement is introduced to perform local mesh refining process within the regions that have relatively large approximation errors.

The *a posteriori* error estimation for the  $\mathbf{H}(\mathbf{curl})$  problem in (1.1) with constant or continuous coefficients has been studied recently by several researchers. Several types of *a posteriori* error estimators have been introduced and analyzed. These include residual-based estimators and the corresponding convergence analysis (explicit [3, 29, 31, 34, 12, 13, 14], and implicit [22]), equilibrated estimators [5], and recovery-based estimators [30]. It is interesting to note that there are four types of errors in the explicit residual-based estimator (see [3]). Two of them are standard, i.e., the element residual and the face jump associated with the original equation in (1.1). The other two are also the element residual and the face jump, but associated with the divergence of the original equation:  $\nabla \cdot (\beta \mathbf{u}) = \nabla \cdot \mathbf{f}$ .

The recovery-based estimator studied in [30] may be viewed as an extension of the popular Zienkiewicz-Zhu (ZZ) error estimator ([40]) for the Poisson equation to the  $\mathbf{H}(\mathbf{curl})$  problem with constant coefficients. More specifically, two quantities related to the solution  $\mathbf{u}$  and  $\nabla \times \mathbf{u}$  are recovered based on the current approximation of the solution in a richer recovery space. The recovery space in [30] is the *continuous* piecewise polynomial space, and the recovery procedure is done through averaging on vertex patches. The resulting ZZ estimator consisting of two terms is shown to be equivalent to the face jumps across the element faces. The element residuals are not included in the estimator in [30].

The purpose of this paper is to develop and analyze an efficient, reliable, and robust recovery-based *a posteriori* error estimator for the finite element approximation

to the  $\mathbf{H}(\mathbf{curl})$  interface problem, i.e., problem (1.1) with piecewise constant coefficients. Theoretically, the efficiency refers that the local error indicator is bounded above by the local error, the reliability refers that the global error is bounded above by the global estimator. The robustness refers that constants in the efficiency and the reliability bounds are independent of the jumps of the coefficients.

The recovered-based estimator introduced in this paper may be viewed as an extension of our previous work in [7, 8] on the diffusion interface problem to the  $\mathbf{H}(\mathbf{curl})$  interface problem, which partially resolve the non-robustness of ZZ error estimator for interface problems. Specifically, we recover two quantities related to  $\mu^{-1}\nabla \times \mathbf{u}$  and  $\beta\mathbf{u}$  in the respective  $\mathbf{H}(\mathbf{curl})$ - and  $\mathbf{H}(\mathbf{div})$ -conforming finite element spaces (the lowest order Nédélec and Brezzi-Douglas-Marini elements respectively). For discussions on which quantities to be recovered and in what finite element spaces, see [7, 8]. The resulting estimator measures the face jumps of the tangential components and the normal component of the numerical approximations to  $\mu^{-1}\nabla \times \mathbf{u}$  and  $\beta\mathbf{u}$ , respectively. Our study indicates that the element residual is no longer higher order than the rest terms in the estimator, the contrary of which is proved to be the case in the diffusion problem ([10]). As a result, the element residual using recovered quantities is part of our proposed error estimator as well.

Theoretically proving a robust reliability bound for the  $\mathbf{H}(\mathbf{curl})$  interface problem is much harder than that for the diffusion interface problem. This is because one needs to estimate the dual norm of the residual functional over the  $\mathbf{H}(\mathbf{curl})$  space. To overcome this difficulty, one needs to use a Helmholtz decomposition of the error (e.g. see [3]). For the  $\mathbf{H}(\mathbf{curl})$  interface problem, additional difficulty is that the decomposition has to be stable under a coefficient weighted norm. To obtain such a decomposition is a non-trivial matter, for the discrete level, a discrete weighted Helmholtz decomposition is studied together with its application and analysis for non-overlapping domain decomposition method in [25]. Here for the continuous version, under certain assumptions, we are able to accomplish this task through establishing a weighted identity relating gradient, curl, and divergence of a piecewisely smooth vector field (see Lemma A.4), which is an extension to the technique used in [17]. The final decomposition result in our paper is similar to the one in [41], the coefficient distribution setting is slightly more general than the one used in [41]. Our proof uses a piecewise regularity result from [18] than directly building from extension in [41].

Another necessary tool for proving a robust reliability bound is a tweaked version of the Clément-type interpolation. We are able to extend naturally from the idea in [4, 33] for the vertex-based continuous Lagrange element to the edge-based Nédélec element in three dimensions. Moreover, our quasi-monotone assumption on the distribution of the coefficients is based on edges which is similar to that of [33] based on vertices in 2D, and our proof borrows the idea from [4]. This is the first Nédélec interpolation known to achieve such a robust bound.

Moving onto the efficiency bound estimate, we prove the every part of the local

recovery-based error estimator can be bounded by the robustly weighted residual-based error estimator. For the local error indicator measuring the irrotational part (gradient part) of the error, using the weighted averaging technique, the constant in the bounds is independent of the coefficient jumps across the interface. For the local estimator measuring the jump of the numerical approximation to  $\mu^{-1}\nabla \times \mathbf{u}$  (weak solenoidal or curl part of the error), the degrees of freedom of the corresponding recovered quantity sits on the edge (lowest order Nédélec elements). Consequently, the averaging is performed on an edge patch in 3D, and this resembles the averaging of Zienkiewicz-Zhu (ZZ) error estimator on vertex patch in 2D. It is known that, if the averaging is done in vertex patches that span across the interface, ZZ error estimator (even correctly weighted) is not robust with respect to the ratio of the max/min of the coefficients on diffusion interface problem (e.g. see [7]). Here for the  $\mathbf{H}(\mathbf{curl})$  interface problem, under the assumption of the quasi-monotone distribution of the coefficients again, we are able to prove that the ZZ type averaging, if carefully weighted, results a robust estimator with respect to the coefficient jump. This is a first known result as well.

Numerically, we are able to show that the recovery-based estimator studied in this paper is more accurate than the residual-based estimator in [3] for several test problems.

This paper is organized as follows. The variational formulation and the  $\mathbf{H}(\mathbf{curl})$ -conforming finite element approximation are introduced in section 2. The explicit recovery procedures and the resulting *a posteriori* error estimators are discussed in section 3. In section 4, the reliability and efficiency bounds are proved along with the technical tools for analysis. The proofs of the bounds for the weighted Helmholtz decomposition is presented in the appendix if certain conditions are met. Finally, some numerical results for the benchmark testing problems are presented in section 5.

## 2 Preliminaries

### 2.1 Notations

Hereby we list some formal definitions concerning problem (1.1). The function space for the variational problem is:

$$\mathbf{H}_g(\mathbf{curl}; \Omega) := \{\mathbf{u} \in \mathbf{H}(\mathbf{curl}; \Omega) : \mathbf{u} \times \mathbf{n} = \mathbf{g} \text{ on } \partial\Omega\}, \quad (2.1)$$

equipped with the  $\mathbf{H}(\mathbf{curl})$  norm

$$\|\mathbf{u}\|_{\mathbf{H}(\mathbf{curl})} = \left( \|\mathbf{u}\|_{\mathbf{L}^2(\Omega)}^2 + \|\nabla \times \mathbf{u}\|_{\mathbf{L}^2(\Omega)}^2 \right)^{1/2}. \quad (2.2)$$

The bilinear form of the variational problem to (1.1) is:

$$\mathcal{A}(\mathbf{u}, \mathbf{v}) := \int_{\Omega} (\mu^{-1} \nabla \times \mathbf{u} \cdot \nabla \times \mathbf{v} + \beta \mathbf{u} \cdot \mathbf{v}) dx, \quad (2.3)$$

and the coefficient-weighted norm related to this problem is:

$$\|\mathbf{u}\|^2 := \mathcal{A}(\mathbf{u}, \mathbf{u}). \quad (2.4)$$

If a subscript is added for the weighted norm, it means the local weighted norm defined on an open subset  $\mathcal{O} \subset \Omega$ :

$$\|\mathbf{u}\|_{\mathcal{O}}^2 := \int_{\mathcal{O}} (\mu^{-1} \nabla \times \mathbf{u} \cdot \nabla \times \mathbf{u} + \beta \mathbf{u} \cdot \mathbf{u}) d\mathbf{x}. \quad (2.5)$$

In addition to the standard  $\mathbf{H}(\text{div})$  space (1.3), we need the weighted version as well:

$$\mathbf{H}(\text{div } \alpha; \Omega) = \{\mathbf{v} \in \mathbf{L}^2(\Omega) : \nabla \cdot (\alpha \mathbf{v}) \in L^2(\Omega) \text{ in } \Omega\}. \quad (2.6)$$

Let  $\mathcal{T}_h = \cup\{K\}$  be a triangulation of  $\Omega$  using tetrahedra elements. The sets of all the vertices, edges, and faces of this triangulation are denoted by  $\mathcal{N}_h$ ,  $\mathcal{E}_h$ , and  $\mathcal{F}_h$ , respectively. Denote the vertices, edges, and faces being subsets or elements of a geometric object  $\mathcal{M}$  by  $\mathcal{N}_h(\mathcal{M})$ ,  $\mathcal{E}_h(\mathcal{M})$ , and  $\mathcal{F}_h(\mathcal{M})$ , where  $\mathcal{M}$  can be an element from the objects in the simplicial complex of the triangulation like a specified element  $K$ , or the whole boundary  $\partial\Omega$ , etc. For any vertex  $\mathbf{z} \in \mathcal{N}_h$ , let  $\lambda_{\mathbf{z}}$  be the nodal basis function of continuous piecewise linear element associated with the vertex  $\mathbf{z}$ .

A fixed unit normal vector  $\mathbf{n}_F$  is assigned to each face  $F$ , and a fixed unit tangential vector  $\mathbf{t}_e$  to each edge  $e$ . For any scalar- or vector-valued function  $v$ , define  $\llbracket v \rrbracket_F = v^- - v^+$  on an interior face  $F \in \mathcal{F}_h$  with a fixed unit normal vector  $\mathbf{n}_F$ , where  $v^{\pm} = \lim_{\epsilon \rightarrow 0^{\pm}} v(\mathbf{x} + \epsilon \mathbf{n}_F)$ . Define  $\{v\}_F = (v^+ + v^-)/2$  as the average on this face  $F$ . If  $F$  is a boundary face, the function  $v$  is extended by zero outside the domain to compute  $\llbracket v \rrbracket_F$  and  $\{v\}_F$ .

The following algebraic identity is handy later in proving identities involving interfaces for any scalar- or vector-valued quantities  $a$  and  $b$ :

$$\llbracket ab \rrbracket_F = \{a\}_F \llbracket b \rrbracket_F + \llbracket a \rrbracket_F \{b\}_F. \quad (2.7)$$

Denote the diameter of an element  $K \in \mathcal{T}_h$  by  $h_K$  and the diameter of a face  $F \in \mathcal{F}_h$  by  $h_F$ . We assume that the triangulation  $\mathcal{T}_h$  is shape regular (see [15]), and this assumption holds for any tetrahedron during the local mesh refining process.

The following notations serve as the languages to describe the local element or face patches. They will be used later in local weighted recovery procedure (Section 3), and in the proof of estimates for the weighted Clément-type interpolation (Section 4).

For a face  $F \in \mathcal{F}_h$ , let  $\omega_F$  be the patch of the tetrahedra sharing this face  $F$ . Let  $\omega_{K,F}$  be the patch of the tetrahedra sharing a face with  $K$ .

For an edge  $e \in \mathcal{E}_h$ , denote by

$$\omega_e = \bigcup_{\{K \in \mathcal{T}_h : e \in \mathcal{E}_h(K)\}} K$$

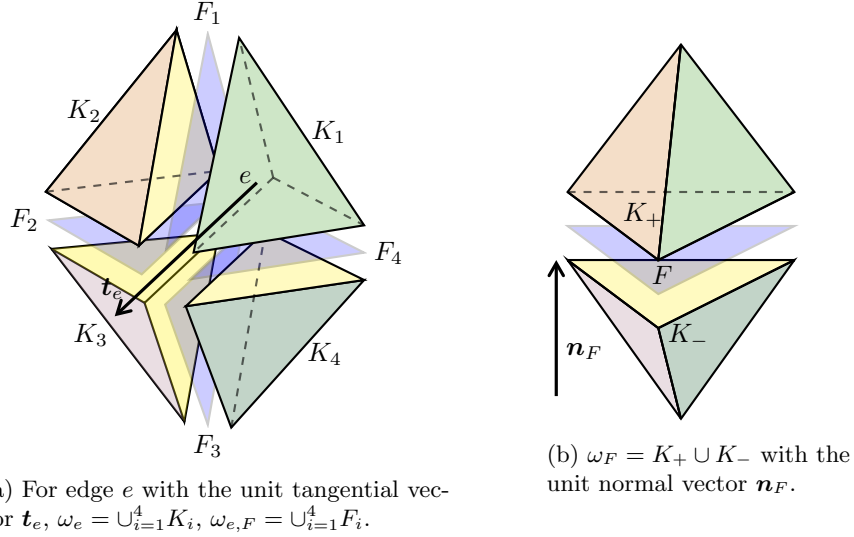


Figure 1: A dissection view of the local edge patch  $\omega_e$ ,  $\omega_{e,F}$ , and face patch  $\omega_F$

the collection of all elements having  $e$  as a common edge, where  $\mathcal{E}_h(K)$  is the collection of edges of the element  $K$ . For the edge patch  $\omega_e$ , we define two  $\mu$ -weighted edge patches associated with an edge  $e \in \mathcal{E}_h$ , which can be understood as the collection of the elements with the biggest/smallest  $\mu^{-1}$  on an edge patch, are referred to

$$\begin{aligned} \tilde{\omega}_e &= \bigcup_{K \in \mathcal{I}_e} K, \quad \text{where } \mathcal{I}_e = \{K \subset \omega_e : \mu_K^{-1} = \max_{K' \subset \omega_e} \mu_{K'}^{-1}\}, \\ \text{and } \hat{\omega}_e &= \bigcup_{K \in \mathcal{I}_e} K, \quad \text{where } \mathcal{I}_e = \{K \subset \omega_e : \mu_K^{-1} = \min_{K' \subset \omega_e} \mu_{K'}^{-1}\}. \end{aligned} \quad (2.8)$$

Denote the union of the interior faces within an edge patch as follows:

$$\omega_{e,F} = \bigcup_{F \in \mathcal{F}_h(\omega_e)} F \setminus \partial \omega_e. \quad (2.9)$$

Using Figure 1 as an illustration,  $\omega_{e,F} = \bigcup_{i=1}^4 F_i$ . Define the  $\mu$ -weighted patch of interior faces as follows:

$$\hat{\omega}_{e,F} = \bigcup_{F \in \mathcal{I}_e} F, \quad \text{where } \mathcal{I}_e = \{F \in \mathcal{F}_h(\hat{\omega}_e) : F \subset \omega_{e,F}\}. \quad (2.10)$$

Taking Figure 1 as an example again, if  $\hat{\omega}_e = K_1 \cup K_2$ , then  $\hat{\omega}_{e,F} = F_1 \cup F_2 \cup F_4$ .

For an element  $K \in \mathcal{T}_h$ , denote the patch of all elements sharing an edge with  $K$  by

$$\omega_{K,e} = \bigcup_{K \in \mathcal{I}_{K,e}} K, \quad \text{where } \mathcal{I}_{K,e} = \{K \in \mathcal{T}_h : K \subset \omega_e \text{ with } e \in \mathcal{E}_h(K)\}. \quad (2.11)$$

Similarly, for a vertex  $z \in \mathcal{N}_h$ , denote by

$$\omega_z = \bigcup_{\{K \in \mathcal{T}_h : z \in \mathcal{N}_h(K)\}} K$$

the collection of all elements having  $\mathbf{z}$  as a common vertex. For the vertex patch  $\omega_{\mathbf{z}}$ , the  $\beta$ -weighted edge patch associated with an vertex  $\mathbf{z} \in \mathcal{N}_h$  is referred to

$$\tilde{\omega}_{\mathbf{z}} = \bigcup_{K \in \mathcal{I}_{\mathbf{z}}} K, \quad \text{where } \mathcal{I}_{\mathbf{z}} = \{K \subset \omega_{\mathbf{z}} : \beta_K = \max_{K \subset \omega_{\mathbf{z}}} \beta_K\}. \quad (2.12)$$

For an element  $K \in \mathcal{T}_h$ , denote the patch of all elements sharing a vertex with  $K$  by

$$\omega_{K,\mathbf{z}} = \bigcup_{K \in \mathcal{I}_{K,\mathbf{z}}} K, \quad \text{where } \mathcal{I}_{K,\mathbf{z}} = \{K \in \mathcal{T}_h : K \subset \omega_{\mathbf{z}} \text{ with } \mathbf{z} \in \mathcal{N}_h(K)\}. \quad (2.13)$$

## 2.2 Finite Element Approximation

The corresponding variational formulation of (1.1) is

$$\begin{cases} \text{Find } \mathbf{u} \in \mathbf{H}_g(\mathbf{curl}; \Omega) \text{ such that:} \\ \mathcal{A}(\mathbf{u}, \mathbf{v}) = (\mathbf{f}, \mathbf{v}), \quad \forall \mathbf{v} \in \mathbf{H}_0(\mathbf{curl}; \Omega), \end{cases} \quad (2.14)$$

where  $(\cdot, \cdot)$  is the standard  $\mathbf{L}^2(\Omega)$ -inner product. Because of  $\mu$  and  $\beta$  being uniformly positive on the domain, the coefficient-weighted norm (2.4) is equivalent to the graph norm (2.2) for  $\mathbf{H}(\mathbf{curl}; \Omega)$ . Moreover the bilinear form (2.3) is intrinsically coercive with respect to this norm. By the Lax-Milgram lemma, there exists a unique solution in  $\mathbf{H}_g(\mathbf{curl}; \Omega)$  to problem (2.14) when the boundary data is “admissible”.

The solution  $\mathbf{u}$  of (2.14) is approximated in a  $\mathbf{H}(\mathbf{curl}; \Omega)$ -conforming finite element space: the lowest order Nédélec finite element space  $\mathcal{ND}_0$  (see [28]). On each element  $K$ , define

$$\mathcal{ND}_0(K) = \{\mathbf{p}(\mathbf{x}) \in \mathbf{P}_1(K) : \mathbf{p} = \mathbf{a} + \mathbf{b} \times \mathbf{x}, \mathbf{a}, \mathbf{b} \in \mathbb{R}^3\}.$$

The global finite element space  $\mathcal{ND}_0$  is glued together through the continuity condition of  $\mathbf{H}(\mathbf{curl}; \Omega)$ :

$$\mathcal{ND}_0 = \{\mathbf{p} \in \mathbf{H}(\mathbf{curl}; \Omega) : \mathbf{p}(\mathbf{x})|_K \in \mathcal{ND}_0(K) \quad \forall K \in \mathcal{T}_h\}.$$

For simplicity, we assume that the Dirichlet boundary data can be represented as the tangential trace of an  $\mathcal{ND}_0$  vector field, i.e.,  $\mathbf{g} = \mathbf{p} \times \mathbf{n}$  on the boundary, where  $\mathbf{p} \in \mathcal{ND}_0$ . The finite element approximation is

$$\begin{cases} \text{Find } \mathbf{u}_h \in \mathcal{ND}_0 \cap \mathbf{H}_g(\mathbf{curl}; \Omega) \text{ such that:} \\ \mathcal{A}(\mathbf{u}_h, \mathbf{v}_h) = (\mathbf{f}, \mathbf{v}_h), \quad \forall \mathbf{v}_h \in \mathcal{ND}_0 \cap \mathbf{H}_0(\mathbf{curl}; \Omega). \end{cases} \quad (2.15)$$

The problem in (2.15) is well-posed in its own right.

Before building the error estimator, we need an  $\mathbf{H}(\mathbf{div}; \Omega)$ -conforming finite element space  $\mathcal{BDM}_1$ , which is the linear order Brezzi-Douglas-Marini face element

(see [6]). On each element  $K$ , define, in a way that leads to the local basis construction,

$$\mathcal{BDM}_1(K) = \{\mathbf{p}(\mathbf{x}) \in \mathbf{P}_1(K) : \mathbf{p} = \mathbf{a} + c\mathbf{x} + \nabla \times (b\mathbf{s}), \mathbf{a}, \mathbf{s} \in \mathbb{R}^3, c \in \mathbb{R}^1, b \in B(K)\},$$

where  $B(K)$  the space of quadratic edge bubble functions in  $K$ . Similarly the global  $\mathcal{BDM}_1$  inherits the continuity condition from  $\mathbf{H}(\text{div}; \Omega)$ :

$$\mathcal{BDM}_1 = \{\mathbf{p} \in \mathbf{H}(\text{div}; \Omega) : \mathbf{p}(\mathbf{x})|_K \in \mathcal{BDM}_1(K) \quad \forall K \in \mathcal{T}_h\}.$$

Let  $K \in \mathcal{T}_h$  be an arbitrary tetrahedral element with vertices  $\mathbf{z}_i, \mathbf{z}_j, \mathbf{z}_k$ , and  $\mathbf{z}_l$ , and let  $\mathbf{n}_i$  be the outer unit vector normal to the face  $F_i = \text{conv}(\mathbf{z}_j \mathbf{z}_k \mathbf{z}_l)$ , opposite to the vertex  $\mathbf{z}_i$ . Let  $\mathbf{t}_{ij}$  be the unit vector of the edge  $e_{ij}$  orienting in the direction of  $\mathbf{z}_j - \mathbf{z}_i$ . The  $\mathcal{ND}_0$  nodal basis function for the edge  $e_{ij}$  can be written as (e.g. see [35, 37]):

$$\varphi_{e_{ij}} = \frac{\lambda_i \mathbf{n}_j}{\mathbf{t}_{ij} \cdot \mathbf{n}_j} - \frac{\lambda_j \mathbf{n}_i}{\mathbf{t}_{ij} \cdot \mathbf{n}_i}, \quad (2.16)$$

where  $\lambda_n$  for  $n = i, j, k, l$  are the barycentric coordinates associated with the vertex  $\mathbf{z}_n$  satisfying  $\lambda_i + \lambda_j + \lambda_k + \lambda_l = 1$ . The degree of freedom of  $\mathcal{ND}_0$  can be then associated with each edge  $e \in \mathcal{E}_h$ , in that  $\varphi_e$  satisfies

$$\varphi_e \cdot \mathbf{t}_{e'}|_{e'} = \frac{1}{|e'|} \int_{e'} \varphi_e \cdot \mathbf{t}_{e'} \, ds = \pm \delta_{ee'}, \quad \forall e' \in \mathcal{E}_h(K),$$

where  $\delta_{ee'}$  is the Kronecker delta. The plus sign is taken when locally  $\mathbf{t}_e$ 's direction coincides with the globally fixed  $\mathbf{t}_{e'}$ 's.

Similarly, we cook up a customized version of the  $\mathcal{BDM}_1$  nodal basis function associated with the vertex  $\mathbf{z}_j$  on face  $F_i$  as follows

$$\psi_{F_i, \mathbf{z}_j} = 9 \frac{\lambda_j \mathbf{t}_{ij}}{\mathbf{n}_i \cdot \mathbf{t}_{ij}} - 3 \frac{\lambda_k \mathbf{t}_{ik}}{\mathbf{n}_i \cdot \mathbf{t}_{ik}} - 3 \frac{\lambda_l \mathbf{t}_{il}}{\mathbf{n}_i \cdot \mathbf{t}_{il}}. \quad (2.17)$$

Now the degrees of freedom of  $\mathcal{BDM}_1$  can be defined using the first moment on  $F_i$  because  $\psi_{F_i, \mathbf{z}_j}$  satisfies:

$$\frac{1}{|F_i|} \int_{F_i} (\psi_{F_i, \mathbf{z}_j} \cdot \mathbf{n}_{F_i}) \lambda_{\mathbf{z}_m} \, dS = \pm \delta_{jm}, \quad \text{for } m \in \{j, k, l\},$$

and  $\psi_{F_i, \mathbf{z}_j} \cdot \mathbf{n}_{F'} = 0$  for any face  $F' \in \mathcal{F}_h(K)$  other than  $F_i$ . Similarly, the plus sign is taken when locally the exterior unit normal  $\mathbf{n}_i$  to face  $F_i$  is in the same direction with the globally fixed unit normal  $\mathbf{n}_{F_i}$ .

### 3 The Recovery-type Error Estimator

There are two important physical quantities of interest: the magnetic field intensity and displacement current density which are related to the electric field intensity  $\mathbf{u}$ . The magnetic field intensity at current time step is denoted by  $\boldsymbol{\sigma}$ , and displacement current density diluted by the time step size is denoted by  $\boldsymbol{\tau}$ . For  $\mathbf{H}(\mathbf{curl})$  problem (1.1) that is time-independent, they can be represented by the following

$$\boldsymbol{\sigma} = \mu^{-1} \nabla \times \mathbf{u} \quad \text{and} \quad \boldsymbol{\tau} = \beta \mathbf{u}, \quad (3.1)$$

then the partial differential equation in (1.1) can be rewritten as

$$\nabla \times \boldsymbol{\sigma} + \boldsymbol{\tau} = \mathbf{f}. \quad (3.2)$$

By the assumption of the data  $\mathbf{f} \in \mathbf{H}(\text{div}; \Omega)$ , it is straightforward to verify that the  $\mathbf{u}$ ,  $\boldsymbol{\sigma}$ , and  $\boldsymbol{\tau}$  lie in the following spaces

$$\begin{aligned} \mathbf{u} &\in \mathbf{H}(\mathbf{curl}; \Omega), \quad \boldsymbol{\tau} \in \mathbf{H}(\text{div}; \Omega), \\ \text{and } \boldsymbol{\sigma} &\in \mathbf{H}(\mathbf{curl}; \Omega) \cap \mathbf{H}(\text{div } \mu; \Omega), \end{aligned} \quad (3.3)$$

where the weighted space  $\mathbf{H}(\text{div } \mu; \Omega)$  is defined in (2.6).

The relation (3.3) indicates the continuity conditions  $\mathbf{u}$ ,  $\boldsymbol{\sigma}$ , and  $\boldsymbol{\tau}$  must fulfill in the continuous level in (3.1) and (3.2). These continuity requirements not just come from the operator theory in Hilbert spaces, but also translate from the original Maxwell equations. For an arbitrary interface  $S$  within the domain, if there is no surface charge on  $S$ , it is well known from physics (e.g., see [27]) that

$$[\![\mathbf{u} \times \mathbf{n}]\!]_S = \mathbf{0}, \quad [\![\boldsymbol{\sigma} \times \mathbf{n}]\!]_S = \mathbf{0}, \quad [\![\mu \boldsymbol{\sigma} \cdot \mathbf{n}]\!]_S = 0, \quad \text{and} \quad [\![\boldsymbol{\tau} \cdot \mathbf{n}]\!]_S = 0. \quad (3.4)$$

These zero-jump conditions are consistent with the continuity conditions for  $\mathbf{H}(\mathbf{curl})$  and  $\mathbf{H}(\text{div})$ , respectively. However, during rendering the continuous problem into the finite element approximation, numerical magnetic field intensity and numerical displacement current density,

$$\boldsymbol{\sigma}_h := \mu^{-1} \nabla \times \mathbf{u}_h \quad \text{and} \quad \boldsymbol{\tau}_h := \beta \mathbf{u}_h,$$

violate the second and the last continuity conditions from (3.4), respectively. Therefore, two quantities are recovered in the respective  $\mathbf{H}(\mathbf{curl})$ -conforming and  $\mathbf{H}(\text{div})$ -conforming finite element spaces using an explicit local weighted averaging technique. Note that the normal component of  $\boldsymbol{\tau}_h$  is a piecewise polynomial of degree one on each face. Consequently, we need to use either  $\mathbf{BDM}_1$  or  $\mathbf{RT}_1$  for recovering displacement current density, instead of  $\mathbf{RT}_0$ .

### 3.1 Local Recovery Procedure

We recover two quantities,  $\boldsymbol{\sigma}_h^*$  and  $\boldsymbol{\tau}_h^*$ , based on  $\boldsymbol{\sigma}_h$  and  $\boldsymbol{\tau}_h$  through weighted averaging locally on edge and face patches, respectively. To this end, for a fixed interior face  $F \subset \mathcal{F}_h$ , denote by  $K_{\pm}$  the neighboring tetrahedra sharing this  $F$  as a common face. Recall that  $\mathbf{n}_F$  is the fixed unit vector normal to the face  $F$ , let  $K_+$  be the tetrahedron with  $\mathbf{n}_F$  as its inward normal, and  $K_-$  with  $\mathbf{n}_F$  as its outward normal (see Figure 1). Let

$$\gamma_F^- = \frac{\mu_{K_+}^{-1/2}}{\mu_{K_-}^{-1/2} + \mu_{K_+}^{-1/2}} \text{ and } \kappa_F^- = \frac{\beta_{K_+}^{1/2}}{\beta_{K_-}^{1/2} + \beta_{K_+}^{1/2}}, \quad (3.5)$$

and  $\gamma_F^+ = 1 - \gamma_F^-$ ,  $\kappa_F^+ = 1 - \kappa_F^-$ . If  $F$  is a boundary face with its neighboring tetrahedron  $K_-$ , we set  $\gamma_F^+ = \kappa_F^+ = 1$  and  $\gamma_F^- = \kappa_F^- = 0$ .

The local averages  $\boldsymbol{\sigma}_{h,F}$  and  $\boldsymbol{\tau}_{h,F}$  on face  $F$  are chosen using the weights above:

$$\boldsymbol{\sigma}_{h,F} = \gamma_F^- \boldsymbol{\sigma}_{h,K_-} + \gamma_F^+ \boldsymbol{\sigma}_{h,K_+} \text{ and } \boldsymbol{\tau}_{h,F} = \kappa_F^- \boldsymbol{\tau}_{h,F_-} + \kappa_F^+ \boldsymbol{\tau}_{h,F_+} \quad (3.6)$$

respectively, where  $\boldsymbol{\sigma}_{h,K_{\pm}} = \boldsymbol{\sigma}_h|_{K_{\pm}}$ , and  $\boldsymbol{\tau}_{h,F_{\pm}}(\mathbf{x}) = \lim_{\epsilon \rightarrow 0^{\pm}} \boldsymbol{\tau}_h(\mathbf{x} + \epsilon \mathbf{n}_F)$  on face  $F$ . The notation discrepancy in above construction is due to the fact, which is mentioned earlier in previous subsection, that  $\boldsymbol{\tau}_h$ 's normal component on each face is a linear polynomial, yet  $\boldsymbol{\sigma}_h$  is a constant vector on a fixed  $K$ .

Now we construct the recovered quantities  $\boldsymbol{\sigma}_h^*$  and  $\boldsymbol{\tau}_h^*$  from the above local averages of  $\boldsymbol{\sigma}_h$  and  $\boldsymbol{\tau}_h$  as follows:

$$\boldsymbol{\sigma}_h^*(\mathbf{x}) = \sum_{e \in \mathcal{E}_h} \left\{ \sum_{F \subset \widehat{\omega}_{e,F}} \left( \frac{1}{|\widehat{\omega}_{e,F}|} \int_F (\boldsymbol{\sigma}_{h,F} \cdot \mathbf{t}_e) dS \right) \right\} \boldsymbol{\varphi}_e(\mathbf{x}) \quad (3.7)$$

$$\text{and } \boldsymbol{\tau}_h^*(\mathbf{x}) = \sum_{F \in \mathcal{F}_h} \sum_{\mathbf{z} \in \mathcal{N}_h(F)} \left( \frac{1}{|F|} \int_F (\boldsymbol{\tau}_{h,F} \cdot \mathbf{n}_F) \lambda_{\mathbf{z}} dS \right) \boldsymbol{\psi}_{F,\mathbf{z}}(\mathbf{x}),$$

where  $\boldsymbol{\varphi}_e \in \mathcal{ND}_0$  and  $\boldsymbol{\psi}_{F,\mathbf{z}} \in \mathcal{BDM}_1$  are the nodal basis functions associated with the respective edge  $e$  and vertex  $\mathbf{z}$  on face  $F$  (see (2.16) and (2.17)).

By the construction of the basis functions in (2.16) and (2.17), we can see  $\boldsymbol{\sigma}_h^* \in \mathbf{H}(\mathbf{curl}; \Omega)$  and  $\boldsymbol{\tau}_h^* \in \mathbf{H}(\mathbf{div}; \Omega)$ , respectively. The degrees of freedom of  $\boldsymbol{\tau}_h^*$  are the weighted averages of  $\boldsymbol{\tau}_h := \beta \mathbf{u}_h$  on a face patch. The degrees of freedom of  $\boldsymbol{\sigma}_h^*$  is the weighted averages of  $\boldsymbol{\sigma}_h := \mu^{-1} \nabla \times \mathbf{u}_h$  on selected interior faces in an edge patch.

Now we may define the local error indicator  $\eta_K^2 = \eta_{K,\perp}^2 + \eta_{K,0}^2 + \eta_{K,R}^2$  based on

these averages plus the recovery-type element residual:

$$\begin{aligned}\eta_{K,\perp} &= \left\| \mu^{1/2} \boldsymbol{\sigma}_h^* - \mu^{-1/2} \nabla \times \mathbf{u}_h \right\|_{\mathbf{L}^2(K)}, \quad \eta_{\perp}^2 = \sum_{K \in \mathcal{T}_h} \eta_{K,\perp}^2, \\ \eta_{K,0} &= \left\| \beta^{-1/2} \boldsymbol{\tau}_h^* - \beta^{1/2} \mathbf{u}_h \right\|_{\mathbf{L}^2(K)}, \quad \eta_0^2 = \sum_{K \in \mathcal{T}_h} \eta_{K,0}^2, \\ \eta_{K,R} &= \mu_K^{1/2} h_K \left\| \mathbf{f} - \beta \mathbf{u}_h - \nabla \times \boldsymbol{\sigma}_h^* \right\|_{\mathbf{L}^2(K)}, \quad \text{and } \eta_R^2 = \sum_{K \in \mathcal{T}_h} \eta_{K,R}^2.\end{aligned}\tag{3.8}$$

The global error estimator is defined by  $\eta^2 = \eta_{\perp}^2 + \eta_0^2 + \eta_R^2$ .

## 4 Reliability and Efficiency Bounds

This section studies the reliability and efficiency of the estimators defined in the previous section. The efficiency bound of the local indicator is established in section 4.4. To prove the reliability bound of the global estimator, we need two tools: (1) a Helmholtz decomposition with weighted norm estimate section 4.1, for detailed proof under certain assumption please see Appendix A) that splits the error into two parts, and (2) a modified Clément-type interpolation (section 4.2). Under the assumption of a robust weighted Helmholtz decomposition exists, two quasi-monotonicity assumptions on the distribution of the coefficients, the reliability bound is obtained in section 4.3, and it is uniform with respect to the jumps of the coefficients.

### 4.1 Helmholtz Decomposition

For any vector in  $\mathbf{H}_0(\mathbf{curl}; \Omega)$ , there exists an orthogonal decomposition with respect to the bilinear form  $\mathcal{A}(\cdot, \cdot)$  (see [18, 20]). This weighted splitting was used in [3] for continuously differentiable  $\mu$  and  $\beta$  to prove the reliability bound of a residual-based a posteriori error estimator. Here we first present the robust weighted splitting result as an assumption (Assumption 4.1), then in Appendix A we show the proof of a bound independent of the coefficient jump ratio, under certain assumptions about the geometries and the relations between coefficients.

Define the  $\mathbf{X}(\Omega, \beta)$  as the space of curl-integrable functions intersecting weighted div-integrable vector fields, and  $\mathbf{PH}^s(\Omega, \mathcal{P})$  as the space of *piecewisely continuous* vector fields on each subdomain:

$$\begin{aligned}\mathbf{X}(\Omega, \beta) &= \mathbf{H}(\operatorname{div} \beta; \Omega) \cap \mathbf{H}_0(\mathbf{curl}; \Omega), \\ \text{and } \mathbf{PH}^s(\Omega, \mathcal{P}) &= \{ \mathbf{v} \in \mathbf{L}^2(\Omega) : \mathbf{v}|_{\Omega_j} \in \mathbf{H}^s(\Omega_j), j = 1, \dots, m \}.\end{aligned}\tag{4.1}$$

**Assumption 4.1** (Weighted Helmholtz decomposition). *We assume that for any  $\mathbf{v} \in \mathbf{H}_0(\mathbf{curl}; \Omega)$ , there exist  $\psi \in H_0^1(\Omega)$  and  $\mathbf{w} \in \mathbf{PH}^1(\Omega, \mathcal{P}) \cap \mathbf{X}(\Omega, \beta)$  such that the following decomposition holds*

$$\mathbf{v} = \mathbf{w} + \nabla \psi. \tag{4.2}$$

Moreover, the following estimate holds:

$$\sum_{j=1}^m \left\| \mu^{-1/2} \nabla \mathbf{w} \right\|_{\mathbf{L}^2(\Omega_j)} + \left\| \beta^{1/2} \mathbf{w} \right\|_{\mathbf{L}^2(\Omega)} + \left\| \beta^{1/2} \nabla \psi \right\|_{\mathbf{L}^2(\Omega)} \leq C \|\mathbf{v}\|. \quad (4.3)$$

## 4.2 Clément-type Nédélec Interpolation

Weighted Clément-type interpolation operators for nodal Lagrange elements are studied in [4, 33]. Stability and approximation properties of this type of operators are often used in proving a robust reliability bound for a posteriori error estimators. For Nédélec elements, the standard unweighted quasi-interpolations for Nédélec elements are studied in [3, 31, 34]. In [3], the author defines the edge degrees of freedom by averaging on a certain face where that edge lies, which is similar to the construction of the Scott-Zhang interpolation operators. In [31], the averaging is performing on the edge patch consisting of two triangles in 2D. Following the idea of averaging on the weighted vertex patch in [4, 33], and extending the averaging technique on edge patch in [31] to the three dimensional case, we construct a weighted Clément-type Nédélec interpolation operator from  $\mathbf{H}_0(\mathbf{curl}; \Omega)$  to  $\mathcal{ND}_0$ . If the vector field to be interpolated has  $\mathbf{PH}^1(\Omega, \mathcal{P})$  regularity, then the approximation and stability properties of the interpolant are proved to be robust under the weighted norm, with the assumption that the coefficient is quasi-monotone in Assumption 4.4.

First we define the standard Nédélec interpolation in any  $K \in \mathcal{T}_h$ . To make this interpolant well-defined and bounded, we need to restrict that the vector field to be interpolated on each element  $K$  lies in the space  $\mathbf{H}^{1/2+\delta}(K)$  for some  $\delta > 0$ , with its curl in  $\mathbf{L}^p(K)$  for some  $p > 2$  (see [27] Lemma 5.38).

**Definition 4.2** (Nédélec interpolation). For any  $\mathbf{v}|_K \in \mathbf{H}^{1/2+\delta}(K)$  with  $\nabla \times \mathbf{v}|_K \in \mathbf{L}^p(K)$ , define the interpolation operator  $\Pi_h : \mathbf{H}^{1/2+\delta}(K) \rightarrow \mathcal{ND}_0$  on each element  $K \in \mathcal{T}_h$  as follows:

$$\Pi_h \mathbf{v}|_K = \sum_{e \in \mathcal{E}_h(K)} \alpha_e(\mathbf{v}) \varphi_e, \quad \text{with } \alpha_e(\mathbf{v}) = \frac{1}{|e|} \int_e \mathbf{v} \cdot \mathbf{t}_e \, ds.$$

**Definition 4.3** (Weighted Clément-type Nédélec interpolation). For any  $\mathbf{v} \in \mathbf{H}_0(\mathbf{curl}; \Omega)$ , such that  $\mathbf{v}|_{\omega_{K,e}} \in \mathbf{H}(\mathbf{curl}; \omega_{K,e}) \cap \mathbf{PH}^1(\omega_{K,e}, \mathcal{P})$ , define the weighted quasi-interpolation operator  $\tilde{\Pi}_h : \mathbf{L}^2(\Omega) \rightarrow \mathcal{ND}_0$  on each element  $K \in \mathcal{T}_h$  as follows:

$$\tilde{\Pi}_h \mathbf{v}|_K = \sum_{e \in \mathcal{E}_h(K)} \tilde{\alpha}_e(\mathbf{v}) \varphi_e, \quad \text{with } \tilde{\alpha}_e(\mathbf{v}) = \left( \frac{1}{|\tilde{\omega}_e|} \int_{\tilde{\omega}_e} \mathbf{v} \, dx \right) \cdot \mathbf{t}_e$$

if  $e$  is an interior edge, i.e., the 1-dimensional Lebesgue measure  $\text{meas}_1(e \cap \partial\Omega) = 0$ . If  $e \in \mathcal{E}_h(\partial\Omega)$ , then  $\tilde{\alpha}_e(\mathbf{v}) = 0$ .

To establish the stability and approximation bounds for this interpolation uniform with respect to  $\mu^{-1}$ , a quasi-monotonicity assumption is needed on the distribution of the coefficients associated with each edge patch  $\omega_e$  in three dimensions, which is similar to those of [4, 33] associated with each vertex patch in two dimensions. The quasi-monotonicity, in layman's terms, can be phrased as “for every element in an edge patch, there exists a simply-connected element path leading to the element where the coefficient achieves the maximum (or minimum) on this patch”. The following assumption is stated a mathematically rigorous way to convey above idea.

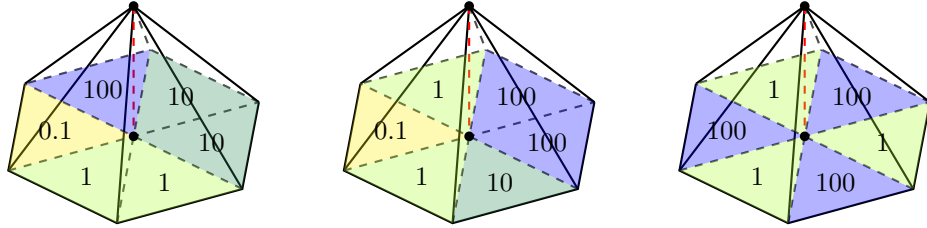
**Assumption 4.4** (Quasi-monotonicity of the  $\mu^{-1}$  in an edge patch). *For each edge  $e \in \mathcal{E}_h$ , if  $e$  is an interior edge, for every  $K \subset \omega_e$ , and every  $K' \subset \tilde{\omega}_e$ , (i) assume that there exist a collection of elements  $\omega'_e = \bigcup_{i=1}^{l(K,e)} K_i \subset \omega_e$  with  $K_{l(K,e)} \subset \tilde{\omega}_e$ , such that  $K_i$  shares a face with  $K_{i-1}$ , and that  $\mu_{K_{i-1}}^{-1} \leq \mu_{K_i}^{-1}$  for all  $i = 1, \dots, l(K,e)$ , where  $K_0 = K$ . If  $e$  is a boundary edge, for every  $K \subset \omega_e \setminus \tilde{\omega}_e$ , and every  $K' \subset \tilde{\omega}_e$ , (ii) assume that (i) holds, and the 2-dimensional Lebesgue measure  $\text{meas}_2(\partial \tilde{\omega}_e \cap \partial \Omega) > 0$ .*

The assumption is phrase using  $\tilde{\omega}_e$ , the assumption remains the same if we switch  $\tilde{\omega}_e$  to  $\hat{\omega}_e$ , and reverse the direction of the inequalities.

If Assumption 4.4 is satisfied, the extended  $\mu$ -weighted patch for an element  $K$  is denoted as

$$\tilde{\omega}_{K,e} = K \bigcup_{e \in \mathcal{E}_h(K)} \omega'_e \bigcup_{e \in \mathcal{E}_h(K)} \tilde{\omega}_e. \quad (4.4)$$

**Remark 4.5.** *Assumption 4.4 (i) is weaker than the extension of the quasi-monotonicity assumption in [4], and is the equivalent to the extension of the quasi-monotonicity assumption in [33] from the vertex patch in two dimensions to the edge patch in three dimensions. Notice if Assumption 4.4 is met, then  $\tilde{\omega}_e$  is a simply connected Lipschitz polyhedron for any interior edge  $e$ .*



(a) Quasi-monotone in the senses of the extension of [4], the extension of [33], and Assumption 4.4.  
(b) Quasi-monotone in the senses of the extension of [33] and Assumption 4.4, not in the extension of [4].  
(c) Not quasi-monotone in any sense.

Figure 2: Different scenarios of the coefficient distribution for  $\mu^{-1}$  for an interior edge patch  $\omega_e$ , where the edge  $e$  is marked as red dotted vertical edge in each figure. The tetrahedra whose bases are marked using blue color in (a) and (b) consist the  $\tilde{\omega}_e$  for this edge patch.

The illustrations in Figure 2 show the difference and similarity between the Assumption 4.4 and the extension to those in [4, 33]. In Figure 2a, for any two tetrahedra in the edge patch  $\omega_e$ , there always exists a monotone path connecting these made of tetrahedra, along which one tetrahedron shares one face with the next tetrahedron in this path. In Figure 2b, along the path from any tetrahedron in this patch to the one with the biggest coefficients  $\mu^{-1}$ , the coefficients are monotone. In Figure 2c, the coefficient distribution of the checkerboard type is not quasi-monotone in any sense, and a Clément-type interpolation can not achieve a robust bound (see [33, 38]), if the edge of interest is an interior edge of the triangulation.

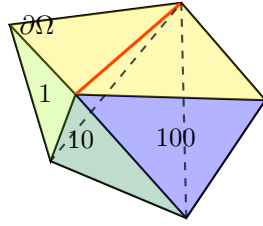
**Theorem 4.6** (Approximation and stability properties). *Under Assumption 4.4, the interpolation operator  $\tilde{\Pi}_h$  in Definition 4.3, satisfies the following estimates:*

$$\begin{aligned} \|\mu^{-1/2}(\mathbf{v} - \tilde{\Pi}_h \mathbf{v})\|_{L^2(K)} &\leq C h_K \|\mu^{-1/2} \nabla \mathbf{v}\|_{L^2(\tilde{\omega}_{K,e})}, \\ \text{and } \|\mu^{-1/2} \nabla \times (\mathbf{v} - \tilde{\Pi}_h \mathbf{v})\|_{L^2(K)} &\leq C \|\mu^{-1/2} \nabla \mathbf{v}\|_{L^2(\tilde{\omega}_{K,e})} \end{aligned} \quad (4.5)$$

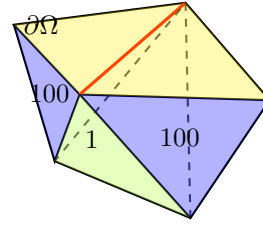
for all  $\mathbf{v} \in \mathbf{H}_0(\mathbf{curl}; \Omega)$  such that  $\mathbf{v}|_{\omega_{K,e}} \in \mathbf{H}(\mathbf{curl}; \omega_{K,e}) \cap \mathbf{PH}^1(\omega_{K,e}, \mathcal{P})$ , where the Jacobian  $\nabla \mathbf{v}$  is defined piecewisely by  $\nabla \mathbf{v}|_K := \nabla(\mathbf{v}|_K)$ .

*Proof.* To establish the inequalities in (4.5), let  $\bar{\mathbf{v}}_K$  and  $\bar{\mathbf{v}}_{\tilde{\omega}_e}$  be the averages of  $\mathbf{v}$  over  $K$  and  $\tilde{\omega}_e$  respectively, i.e.,  $\bar{\mathbf{v}}_K = |K|^{-1} \int_K \mathbf{v} d\mathbf{x}$ , and  $\bar{\mathbf{v}}_{\tilde{\omega}_e} = |\tilde{\omega}_e|^{-1} \int_{\tilde{\omega}_e} \mathbf{v} d\mathbf{x}$  for an interior edge  $e$ . Let  $\bar{\mathbf{v}}_{\tilde{\omega}_e} = \mathbf{0}$  if  $e$  is a boundary edge.

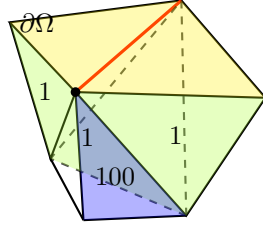
If  $e$  is an interior edge, we have the following standard approximation property (also known as Poincaré inequality) thanks to the shape regularity of the triangulation  $\mathcal{T}_h$ , simply-connectedness of  $\tilde{\omega}_e$  for an interior edge  $e$  from Assumption 4.4, and



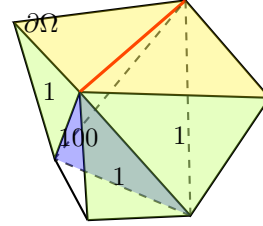
(a) Quasi-monotone in the sense of Assumption 4.4, the extension of [33], and the extension of [4].



(b) Quasi-monotone in the sense of Assumption 4.4 and the extension of [33], not in the sense of the extension of [4].



(c) Quasi-monotone for the edge patch in the sense of Assumption 4.4, not quasi-monotone for vertex patch for the black dotted vertex.



(d) Not quasi-monotone in any sense.

Figure 3: Different scenarios of the coefficient distribution for  $\mu^{-1}$  for a boundary edge patch  $\omega_e$ , where  $e$  is marked red, the boundary faces are marked yellow, and the coefficient in each tetrahedron is marked on its front faces towards the viewer.

$\mathbf{v} \in \mathbf{PH}^1(\omega_{K,e}, \mathcal{P})$ :

$$\|\mathbf{v} - \bar{\mathbf{v}}_K\|_{\mathbf{L}^2(K)} \leq Ch_K \|\nabla \mathbf{v}\|_{\mathbf{L}^2(K)}, \quad \text{and} \quad \|\mathbf{v} - \bar{\mathbf{v}}_{\tilde{\omega}_e}\|_{\mathbf{L}^2(\tilde{\omega}_e)} \leq Ch_e \|\nabla \mathbf{v}\|_{\mathbf{L}^2(\tilde{\omega}_e)}. \quad (4.6)$$

If  $e$  is a boundary edge, the first inequality in (4.6) still holds. To get an equality similar to the second one, the fact that  $\mathbf{v} \in \mathbf{H}_0(\mathbf{curl}; \Omega)$  and  $\mathbf{v}|_{\omega_{K,e}} \in \mathbf{PH}^1(\omega_{K,e}, \mathcal{P})$  implies  $\mathbf{v} \cdot \mathbf{t}_e|_{\tilde{\omega}_e} \in H^1(\tilde{\omega}_e)$ , and  $\mathbf{v} \cdot \mathbf{t}_e|_{\partial \tilde{\omega}_e \cap \partial \Omega} = 0$ . The following Friedrichs inequality holds (even if  $\tilde{\omega}_e$  is not simply-connected as in the case of Figure 3b)

$$\|\mathbf{v} \cdot \mathbf{t}_e\|_{L^2(\tilde{\omega}_e)} \leq Ch_e \|\nabla(\mathbf{v} \cdot \mathbf{t}_e)\|_{L^2(\tilde{\omega}_e)} \leq Ch_e \|\nabla \mathbf{v}\|_{\mathbf{L}^2(\tilde{\omega}_e)}. \quad (4.7)$$

The starting point of the proof is to split the error we want to bound into parts. On any  $K \in \mathcal{T}_h$ , it follows from the triangle inequality that

$$\|\mathbf{v} - \tilde{\Pi}_h \mathbf{v}\|_{\mathbf{L}^2(K)} \leq \|\mathbf{v} - \bar{\mathbf{v}}_K\|_{\mathbf{L}^2(K)} + \|\bar{\mathbf{v}}_K - \tilde{\Pi}_h \mathbf{v}\|_{\mathbf{L}^2(K)}.$$

The first term can be estimated using (4.6) first inequality. For the second term, since  $\tilde{\prod}_h \bar{\mathbf{v}}_K = \bar{\mathbf{v}}_K$  (with slightly abuse of notation we can extend  $\bar{\mathbf{v}}_K$  to whole edge patch by letting it be its value on  $K$ ), we have the following partition on the element  $K$

$$\bar{\mathbf{v}}_K - \tilde{\prod}_h \mathbf{v} = \tilde{\prod}_h (\bar{\mathbf{v}}_K - \mathbf{v}) = \sum_{e \in \mathcal{E}_h(K)} (\bar{\mathbf{v}}_K - \bar{\mathbf{v}}_{\tilde{\omega}_e}) \cdot \mathbf{t}_e \varphi_e.$$

Now applying the triangle inequality, and using the fact that  $\|\varphi_e\|_{L^2(K)} \leq C|K|^{1/2}$  (see the construction of  $\varphi_e$  in (2.16)) yield

$$\begin{aligned} \|\bar{\mathbf{v}}_K - \tilde{\prod}_h \mathbf{v}\|_{L^2(K)} &\leq \sum_{e \in \mathcal{E}_h(K)} \|(\bar{\mathbf{v}}_K - \bar{\mathbf{v}}_{\tilde{\omega}_e}) \cdot \mathbf{t}_e \varphi_e\|_{L^2(K)} \\ &= \sum_{e \in \mathcal{E}_h(K)} |(\bar{\mathbf{v}}_K - \bar{\mathbf{v}}_{\tilde{\omega}_e}) \cdot \mathbf{t}_e| \cdot \|\varphi_e\|_{L^2(K)} \leq C|K|^{1/2} \sum_{e \in \mathcal{E}_h(K)} |(\bar{\mathbf{v}}_K - \bar{\mathbf{v}}_{\tilde{\omega}_e}) \cdot \mathbf{t}_e|. \end{aligned} \quad (4.8)$$

To establish the estimate for  $|(\bar{\mathbf{v}}_K - \bar{\mathbf{v}}_{\tilde{\omega}_e}) \cdot \mathbf{t}_e|$  for each edge, we consider three cases. The first case is that when  $K \subset \tilde{\omega}_e$ , using the triangle inequality, the estimates in (4.6) and (4.7) gives

$$\begin{aligned} |K|^{1/2} |(\bar{\mathbf{v}}_K - \bar{\mathbf{v}}_{\tilde{\omega}_e}) \cdot \mathbf{t}_e| &= \|(\bar{\mathbf{v}}_K - \bar{\mathbf{v}}_{\tilde{\omega}_e}) \cdot \mathbf{t}_e\|_{L^2(K)} \\ &\leq \|(\bar{\mathbf{v}}_K - \mathbf{v}) \cdot \mathbf{t}_e\|_{L^2(K)} + \|(\mathbf{v} - \bar{\mathbf{v}}_{\tilde{\omega}_e}) \cdot \mathbf{t}_e\|_{L^2(K)} \\ &\leq \|\bar{\mathbf{v}}_K - \mathbf{v}\|_{L^2(K)} + \|(\mathbf{v} - \bar{\mathbf{v}}_{\tilde{\omega}_e}) \cdot \mathbf{t}_e\|_{L^2(\tilde{\omega}_e)} \leq C \frac{h_K}{\mu_K^{-1/2}} \|\mu^{-1/2} \nabla \mathbf{v}\|_{L^2(\tilde{\omega}_e)}. \end{aligned}$$

Here the term in front of the last inequality is treated as  $\|(\mathbf{v} - \bar{\mathbf{v}}_{\tilde{\omega}_e}) \cdot \mathbf{t}_e\|_{L^2(\tilde{\omega}_e)} \leq \|\mathbf{v} - \bar{\mathbf{v}}_{\tilde{\omega}_e}\|_{L^2(\tilde{\omega}_e)}$  for an interior edge, and  $\|(\mathbf{v} - \bar{\mathbf{v}}_{\tilde{\omega}_e}) \cdot \mathbf{t}_e\|_{L^2(\tilde{\omega}_e)} = \|\mathbf{v} \cdot \mathbf{t}_e\|_{L^2(\tilde{\omega}_e)}$  for a boundary edge.

The second case is that when  $K \not\subset \tilde{\omega}_e$ , yet  $K$  is adjacent to  $\tilde{\omega}_e$ , and we denote the face they share as  $\partial K \cap \partial \tilde{\omega}_e = F$ . The fact that the tangential component of  $\mathbf{v}$  along the edge  $e$  is continuous across the face  $F$ , and  $\mathbf{v} \in \mathbf{PH}^1(\omega_{K,e}, \mathcal{P})$  imply that  $\mathbf{v} \cdot \mathbf{t}_e \in H^1(K \cup \tilde{\omega}_e \cup F)$  (e.g. see [27] Lemma 5.3). To establish the estimate, we need a standard trace inequality for  $p \in H^1(K \cup \tilde{\omega}_e \cup F)$  (e.g. see [36] Lemma 3.2):

$$\|p\|_{L^2(F)} \leq C \left\{ h_F^{-1/2} \|p\|_{L^2(K')} + h_F^{1/2} \|\nabla p\|_{L^2(K')} \right\}, \quad (4.9)$$

where  $K'$  can be either the element of interest  $K$ , or the element  $\tilde{K}$  as a subset of  $\tilde{\omega}_e$  which is adjacent to  $K$ .

Now it follows from the triangle inequality and shape regularity of the triangulation that

$$\begin{aligned} |K|^{1/2} |(\bar{\mathbf{v}}_K - \bar{\mathbf{v}}_{\tilde{\omega}_e}) \cdot \mathbf{t}_e| &= \frac{|K|^{1/2}}{|F|^{1/2}} \|(\bar{\mathbf{v}}_K - \bar{\mathbf{v}}_{\tilde{\omega}_e}) \cdot \mathbf{t}_e\|_{L^2(F)} \\ &\leq C h_K^{1/2} \|(\bar{\mathbf{v}}_K - \mathbf{v}) \cdot \mathbf{t}_e\|_{L^2(F)} + C h_K^{1/2} \|(\mathbf{v} - \bar{\mathbf{v}}_{\tilde{\omega}_e}) \cdot \mathbf{t}_e\|_{L^2(F)}. \end{aligned} \quad (4.10)$$

The first term in the (4.10) can be estimated using (4.9) and then (4.6)

$$\begin{aligned}
& h_K^{1/2} \|(\bar{\mathbf{v}}_K - \mathbf{v}) \cdot \mathbf{t}_e\|_{L^2(F)} \\
& \leq Ch_K^{1/2} \left\{ h_F^{-1/2} \|(\bar{\mathbf{v}}_K - \mathbf{v}) \cdot \mathbf{t}_e\|_{L^2(K)} + h_F^{1/2} \|\nabla(\mathbf{v} \cdot \mathbf{t}_e)\|_{L^2(K)} \right\} \\
& \leq C \left\{ \|\bar{\mathbf{v}}_K - \mathbf{v}\|_{L^2(K)} + h_K \|\nabla \mathbf{v}\|_{L^2(K)} \right\} \leq Ch_K \|\nabla \mathbf{v}\|_{L^2(K)}.
\end{aligned}$$

For the second term  $h_K^{1/2} \|(\mathbf{v} - \bar{\mathbf{v}}_{\tilde{\omega}_e}) \cdot \mathbf{t}_e\|_{L^2(F)}$  in (4.10), using the same argument yields a similar estimate, except passing the trace inequality from the face  $F$  to the element  $\tilde{K} \subset \tilde{\omega}_e$  this time:

$$h_K^{1/2} \|(\mathbf{v} - \bar{\mathbf{v}}_{\tilde{\omega}_e}) \cdot \mathbf{t}_e\|_{L^2(F)} \leq Ch_{\tilde{K}} \|\nabla \mathbf{v}\|_{L^2(\tilde{\omega}_e)}.$$

Combining the two inequalities obtained above gives the following estimate for any  $e \in \mathcal{E}_h(K)$  thanks to  $\mu_K^{-1} \leq \mu_{\tilde{\omega}_e}^{-1}$ :

$$|K|^{1/2} |(\bar{\mathbf{v}}_K - \bar{\mathbf{v}}_{\tilde{\omega}_e}) \cdot \mathbf{t}_e| \leq C \frac{h_K}{\mu_K^{-1/2}} \|\mu^{-1/2} \nabla \mathbf{v}\|_{L^2(\tilde{\omega}_e)}. \quad (4.11)$$

The third case is that when  $K \not\subset \tilde{\omega}_e$ , nor does  $K$  share a face with  $\tilde{\omega}_e$ . By Assumption 4.4 there is a simply connected patch consisting of  $K_1, \dots, K_{l(K,e)-1}$  along which the  $\mu^{-1}$  is monotone. Separating the term of interest by triangle inequality:

$$|(\bar{\mathbf{v}}_K - \bar{\mathbf{v}}_{\tilde{\omega}_e}) \cdot \mathbf{t}_e| \leq |(\bar{\mathbf{v}}_K - \bar{\mathbf{v}}_{K_1}) \cdot \mathbf{t}_e| + \dots + |(\bar{\mathbf{v}}_{K_{l(K,e)-1}} - \bar{\mathbf{v}}_{\tilde{\omega}_e}) \cdot \mathbf{t}_e|,$$

then each of the above terms can be proved yielding the same form of estimate in (4.11) by the same argument. This result, together with the representation of  $\|\bar{\mathbf{v}}_K - \tilde{\prod}_h \mathbf{v}\|_{L^2(K)}$  in (4.8), implies the first estimate in (4.5).

For the second estimate in (4.5), using the inverse inequality, the triangle inequality, and  $\tilde{\prod}_h \bar{\mathbf{v}}_K = \bar{\mathbf{v}}_K$  again, we have that

$$\begin{aligned}
\|\nabla \times \tilde{\prod}_h \mathbf{v}\|_{L^2(K)} &= \|\nabla \times \tilde{\prod}_h (\mathbf{v} - \bar{\mathbf{v}}_K)\|_{L^2(K)} \leq Ch_K^{-1} \|\tilde{\prod}_h (\mathbf{v} - \bar{\mathbf{v}}_K)\|_{L^2(K)} \\
&\leq Ch_K^{-1} \|\tilde{\prod}_h \mathbf{v} - \mathbf{v}\|_{L^2(K)} + Ch_K^{-1} \|\mathbf{v} - \bar{\mathbf{v}}_K\|_{L^2(K)},
\end{aligned}$$

which, together with the first estimate in (4.5) and (4.6), implies the second estimate. This completes the proof of the theorem.  $\square$

**Assumption 4.7** (Quasi-monotonicity of the  $\beta$  in a vertex patch). *For any vertex  $\mathbf{z} \in \mathcal{N}_h$ , assume that the  $\beta$  satisfies the vertex patch quasi-monotonicity condition in [33]: if  $\mathbf{z}$  is an interior vertex, for any  $K \subset \omega_{\mathbf{z}}$ , and  $K' \subset \tilde{\omega}_{\mathbf{z}}$ , (i) there exist a collection of elements  $\omega'_{\mathbf{z}} = \bigcup_{i=1}^{l(K,\mathbf{z})} K_i \subset \omega_{\mathbf{z}}$  with  $K_{l(K,\mathbf{z})} \subset \tilde{\omega}_{\mathbf{z}}$ , such that  $K_i$  shares a face with  $K_{i-1}$  and that  $\beta_{K_{i-1}} \leq \beta_{K_i}$  for all  $i = 1, \dots, l(K, \mathbf{z})$ , where  $K_0 = K$  and. If  $\mathbf{z}$  is a vertex on the boundary, for every  $K \subset \omega_{\mathbf{z}} \setminus \tilde{\omega}_{\mathbf{z}}$ , and every  $K' \subset \tilde{\omega}_{\mathbf{z}}$ , (ii) assume that (i) holds, and the 2-dimensional Lebesgue measure  $\text{meas}_2(\partial \tilde{\omega}_{\mathbf{z}} \cap \partial \Omega) > 0$ .*

If Assumption 4.7 is satisfied, the extended  $\beta$ -weighted patch for an element  $K$  is denoted as

$$\tilde{\omega}_{K,z} = K \bigcup_{z \in \mathcal{N}_h(K)} \omega'_z \bigcup_{z \in \mathcal{N}_h(K)} \tilde{\omega}_z,$$

For the  $\beta$  which satisfies the vertex patch quasi-monotonicity in Assumption 4.7, the robust Clément-type interpolation for the linear Lagrange elements results are already established in [4, 33]. In the three dimensional setting, one reason to study the Clément-type interpolation is that the standard linear Lagrange nodal interpolant may not be bounded. Unless extra regularity is assumed (e.g. the function to be interpolated is in  $H^{3/2+\epsilon}(\Omega)$ , see [27]), the degrees of freedom for the Lagrange nodal interpolant may not be well-defined because  $H^1(\Omega)$  is not continuously embedded into the continuous function space.

For any  $\psi \in H_0^1(\Omega)$ , let  $\psi_h$  be the weighted Clément-type interpolant of  $\psi$  defined in [33] associated with the coefficient  $\beta$ . Under Assumption 4.7, the  $\psi_h$  has the following properties:

$$\begin{aligned} \left\| \beta^{1/2}(\psi - \psi_h(z)) \lambda_z \right\|_{L^2(K)} &\leq c_1 h_K \left\| \beta^{1/2} \nabla \psi \right\|_{L^2(\tilde{\omega}_{K,z})}, \\ \text{and } \left\| \beta^{1/2} \nabla(\psi - \psi_h) \right\|_{L^2(K)} &\leq c_2 \left\| \beta^{1/2} \nabla \psi \right\|_{L^2(\tilde{\omega}_{K,z})}, \end{aligned} \quad (4.12)$$

for any vertex  $z \in \mathcal{N}_h(K)$ .

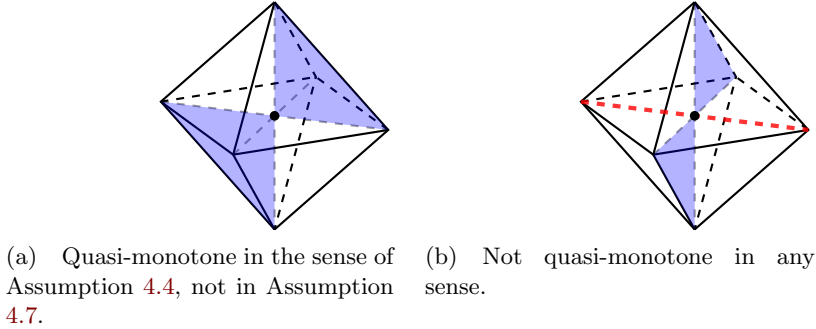


Figure 4: Different scenarios of the coefficient distribution for  $\beta$  for an interior vertex patch  $\omega_z$ . (a)  $\beta = 100$  in the tetrahedra whose faces are marked blue,  $\beta = 1$  in the rest tetrahedra in this patch. The coefficient distribution is quasi-monotone for all interior edges within this patch. (b)  $\beta = 100$  in the four tetrahedra sharing the blue faces,  $\beta = 1$  in the rest tetrahedra in this patch. The quasi-monotonicity is violated for the red edges.

**Remark 4.8.** Assumption 4.4 does not exclude the case when  $\bar{\Omega} = \bar{\Omega}_1 \cup \bar{\Omega}_2$ , and  $\Omega_1$  is a Lipschitz polyhedron touching the boundary at one vertex  $V_1$  only, with

$\mu^{-1}|_{\Omega_1} = 100$ , and  $\mu^{-1}|_{\Omega_2} = 1$ . Assumption 4.7 prohibits the existence of this scenario. In this scenario, a robust Clément-type interpolation can not be achieved for nodal Lagrange elements. However, Assumption 4.4 allows this kind of domain, in which all the edges on the  $\partial\Omega_1$  connecting the vertex  $V_1$  is an interior edge of the triangulation. A robust Clément-type interpolation using Nédélec elements does exist in this scenario. Please refer to the illustration in Figure 3c.

**Remark 4.9.** Assumption 4.4 which states quasi-monotonicity for the edge patch, is weaker than Assumption 4.7 for the vertex patch. The reason is that Assumption 4.4 allows the checkerboard pattern for a vertex patch. However, this vertex patch checkerboard pattern is excluded in Assumption 4.7. Please refer to the illustration in Figure 4. In Figure 4a, the coefficient distribution satisfies Assumption 4.4 for any interior edges within this patch, yet Assumption 4.7 is not met.

### 4.3 Reliability

Under the assumption on the distributions of the coefficients and the Helmholtz decomposition which is stable under the weighted norm, we prove the global reliability for the local recovery error estimator  $\eta$  defined in (3.8).

For any vertex  $\mathbf{z} \in \mathcal{N}_h \setminus \mathcal{N}_h(\partial\Omega)$ , denote by

$$F_{\omega_{\mathbf{z}}} := \frac{1}{|\omega_{\mathbf{z}}|} \int_{\omega_{\mathbf{z}}} \nabla \cdot (\mathbf{f} - \boldsymbol{\tau}_h^*) d\mathbf{x}$$

the average of  $\nabla \cdot (\mathbf{f} - \boldsymbol{\tau}_h^*)$  over the vertex patch  $\omega_{\mathbf{z}}$ . For  $\mathbf{z} \in \mathcal{N}_h(\partial\Omega)$ ,  $F_{\omega_{\mathbf{z}}} := 0$ . Let

$$H = \left( \sum_{K \in \mathcal{T}_h} \eta_{K,d}^2 \right)^{1/2} \quad \text{with} \quad \eta_{K,d} = \beta_K^{-1/2} h_K \|\nabla \cdot (\mathbf{f} - \boldsymbol{\tau}_h^*)\|_{L^2(K)}$$

$$\text{and} \quad \tilde{H} = \left( \sum_{\mathbf{z} \in \mathcal{N}_h} \sum_{K \subset \omega_{\mathbf{z}}} \beta_K^{-1} h_K^2 \|\nabla \cdot (\mathbf{f} - \boldsymbol{\tau}_h^*) - F_{\omega_{\mathbf{z}}}\|_{L^2(K)}^2 \right)^{1/2}.$$

The contribution from interior nodes in  $\tilde{H}$  is a higher order term since  $\nabla \cdot (\mathbf{f} - \boldsymbol{\tau}_h^*) \in L^2(\Omega)$ , and so is the contribution from boundary nodes if  $\nabla \cdot (\mathbf{f} - \boldsymbol{\tau}_h^*) \in L^p(\Omega)$  for some  $p > 2$ . (see [10]).

**Theorem 4.10** (Global Reliability of  $\eta$ ). *Let  $\mathbf{u}$  and  $\mathbf{u}_h$  be the solutions of (2.14) and (2.15), respectively. Under Assumption 4.1, 4.4 and 4.7, there exists a constant  $C > 0$  independent of the jumps of the coefficients such that*

$$\|\mathbf{u} - \mathbf{u}_h\| \leq C(\eta + H). \quad (4.13)$$

*Proof.* Denote the error and the residual by

$$\mathbf{e} = \mathbf{u} - \mathbf{u}_h \quad \text{and} \quad R(\mathbf{v}) = (\mathbf{f}, \mathbf{v}) - (\mu^{-1} \nabla \times \mathbf{u}_h, \nabla \times \mathbf{v}) - (\beta \mathbf{u}_h, \mathbf{v}),$$

respectively. It is easy to see that

$$\mathcal{A}(\mathbf{e}, \mathbf{v}) = R(\mathbf{v}), \quad \forall \mathbf{v} \in \mathbf{H}_0(\mathbf{curl}; \Omega) \quad \text{and} \quad R(\mathbf{v}_h) = 0, \quad \forall \mathbf{v}_h \in \mathcal{ND}_0 \cap \mathbf{H}_0(\mathbf{curl}; \Omega).$$

By Assumption 4.1, there exist a decomposition of the error  $\mathbf{e} \in \mathbf{H}_0(\mathbf{curl}; \Omega)$  into the sum of  $\psi \in H_0^1(\Omega)$  and  $\mathbf{w} \in \mathbf{PH}^1(\Omega, \mathcal{P}) \cap \mathbf{X}(\Omega, \beta)$  such that

$$\mathbf{e} = \mathbf{w} + \nabla \psi \quad \text{and} \quad \|\mathbf{e}\|^2 = R(\mathbf{e}) = R(\mathbf{w}) + R(\nabla \psi).$$

To bound the curl-free part of the error, let  $\psi_h$  be the weighted Clément-type interpolant of  $\psi$  defined in [33] associated with the coefficient  $\beta$ . It follows from the fact that  $R(\nabla \psi_h) = 0$ , integration by parts, the Cauchy-Schwarz inequality, the approximation and stability of the interpolation (4.12), and (4.3) that

$$\begin{aligned} R(\nabla \psi) &= R(\nabla(\psi - \psi_h)) = (\mathbf{f} - \boldsymbol{\tau}_h^*, \nabla(\psi - \psi_h)) + (\boldsymbol{\tau}_h^* - \beta \mathbf{u}_h, \nabla(\psi - \psi_h)) \\ &= -(\nabla \cdot (\mathbf{f} - \boldsymbol{\tau}_h^*), \psi - \psi_h) + (\boldsymbol{\tau}_h^* - \beta \mathbf{u}_h, \nabla(\psi - \psi_h)) \\ &\leq \sum_{K \in \mathcal{T}_h} \left( \eta_{K,d} h_K^{-1} \left\| \beta^{1/2}(\psi - \psi_h) \right\|_{L^2(\omega_{K,z})} + \eta_{K,0} \left\| \beta^{1/2} \nabla(\psi - \psi_h) \right\|_{L^2(\omega_{K,z})} \right) \\ &\leq C \sum_{K \in \mathcal{T}_h} (\eta_{K,d} + \eta_{K,0}) \left\| \beta^{1/2} \nabla \psi \right\|_{L^2(\omega_{K,z})} \leq C (H + \eta_0) \left\| \beta^{1/2} \nabla \psi \right\|_{L^2(\Omega)} \\ &\leq C (H + \eta_0) \left\| \beta^{1/2} \mathbf{e} \right\|_{L^2(\Omega)}. \end{aligned}$$

To bound  $R(\mathbf{w})$ , let  $\mathbf{w}_h = \tilde{\Pi}_h \mathbf{w} \in \mathcal{ND}_0 \cap \mathbf{H}_0(\mathbf{curl}; \Omega)$  with  $\tilde{\Pi}_h$  defined in Definition 4.3. Using the fact that  $R(\mathbf{w}_h) = 0$  and integrating by parts give

$$\begin{aligned} R(\mathbf{w}) &= R(\mathbf{w} - \mathbf{w}_h) \\ &= (\mathbf{f} - \beta \mathbf{u}_h, \mathbf{w} - \mathbf{w}_h) - (\boldsymbol{\sigma}_h^*, \nabla \times (\mathbf{w} - \mathbf{w}_h)) + (\boldsymbol{\sigma}_h^* - \mu^{-1} \nabla \times \mathbf{u}_h, \nabla \times (\mathbf{w} - \mathbf{w}_h)) \\ &= (\mathbf{f} - \beta \mathbf{u}_h - \nabla \times \boldsymbol{\sigma}_h^*, \mathbf{w} - \mathbf{w}_h) + (\boldsymbol{\sigma}_h^* - \mu^{-1} \nabla \times \mathbf{u}_h, \nabla \times (\mathbf{w} - \mathbf{w}_h)). \end{aligned}$$

Now, by the Cauchy-Schwarz inequality, the second and third inequalities in (4.5) , and (4.3), we have

$$\begin{aligned} R(\mathbf{w}) &\leq \sum_{K \in \mathcal{T}_h} \left( \eta_{K,R} h_K^{-1} \left\| \mu^{-1/2}(\mathbf{w} - \mathbf{w}_h) \right\|_{L^2(K)} + \eta_{K,\perp} \left\| \mu^{-1/2} \nabla \times (\mathbf{w} - \mathbf{w}_h) \right\|_{L^2(K)} \right) \\ &\leq C \sum_{K \in \mathcal{T}_h} (\eta_{K,R} + \eta_{K,\perp}) \left\| \mu^{-1/2} \nabla \mathbf{w} \right\|_{L^2(\omega_K)} \leq C (\eta_R + \eta_\perp) \left\| \mu^{-1/2} \nabla \mathbf{w} \right\|_{L^2(\Omega)} \\ &\leq C (\eta_R + \eta_\perp) \left\| \mu^{-1/2} \nabla \times \mathbf{e} \right\|_{L^2(\Omega)}. \end{aligned}$$

Combining the above two inequalities, we have

$$\|\mathbf{e}\|^2 = R(\mathbf{e}) \leq C(\eta + H)\|\mathbf{e}\|,$$

which implies (4.13). This completes the proof of the theorem.  $\square$

In the remainder of this section, we assume that additionally  $\nabla \cdot \mathbf{f} \in L^p(\Omega)$  for some  $p > 2$ , then the  $H$  in (4.13) may be replaced by  $\tilde{H}$  which is a higher order term.

**Theorem 4.11** (Global Reliability of  $\eta$ ). *Under Assumption A.1, 4.4, and 4.7, there exists a constant  $C > 0$  independent of the jumps of the coefficients such that*

$$\|\mathbf{u} - \mathbf{u}_h\| \leq C(\eta + \tilde{H}). \quad (4.14)$$

*Proof.* In the proof of (4.13), if furthermore the following orthogonality condition is exploited on the vertex patch for the weighted Clément-type interpolant (e.g. see [7] Section 4)

$$(1, (\psi - \psi_h(\mathbf{z}))\lambda_{\mathbf{z}})_{\omega_{\mathbf{z}}} = 0, \quad \forall \mathbf{z} \in \mathcal{N}_h \setminus \mathcal{N}_h(\partial\Omega),$$

together with the fact that  $F_{\omega_{\mathbf{z}}} = 0$  and  $\psi_h(\mathbf{z}) = 0$  for  $\mathbf{z} \in \mathcal{N}_h(\partial\Omega)$ , it implies

$$\begin{aligned} (\mathbf{f} - \boldsymbol{\tau}_h^*, \nabla(\psi - \psi_h)) &= - \sum_{K \in \mathcal{T}_h} (\nabla \cdot (\mathbf{f} - \boldsymbol{\tau}_h^*), \psi - \psi_h)_K \\ &= - \sum_{\mathbf{z} \in \mathcal{N}_h} \sum_{K \subset \omega_{\mathbf{z}}} (\nabla \cdot (\mathbf{f} - \boldsymbol{\tau}_h^*) - F_{\omega_{\mathbf{z}}}, (\psi - \psi_h(\mathbf{z}))\lambda_{\mathbf{z}})_K. \end{aligned}$$

Now, a similar argument as in the irrotational part proof of (4.13) gives

$$(\mathbf{f} - \boldsymbol{\tau}_h^*, \nabla(\psi - \psi_h)) \leq C \tilde{H} \|\beta^{1/2} \mathbf{e}\|_{L^2(\Omega)}.$$

The rest of the proof for (4.14) is identical to that of (4.13).  $\square$

#### 4.4 Efficiency

Even though in [3], the coefficients are assumed to be continuous, the proof they used to prove the efficiency bound (Section 4 and 5 in [3]) carries over to piecewise constant coefficients. At the same time, their choice of weight yields a robust bound with no dependence on the coefficients. In this subsection, we prove the efficiency of the recovery-based estimator (3.8) by bounding the recovery-based local error estimator by the residual-based local error estimator.

Let  $\mathbf{f}_h$  be the standard  $\mathbf{L}^2$ -projection onto  $\mathbf{BDM}_1$ . It is proved in [3] that there exists a positive constant  $C$  such that:

$$\begin{aligned} Ch_F \left\| \mu_F^{1/2} \llbracket (\mu^{-1} \nabla \times \mathbf{u}_h) \times \mathbf{n} \rrbracket_F \right\|_{\mathbf{L}^2(F)}^2 &\leq \|\mathbf{u} - \mathbf{u}_h\|_{\omega_F}^2 + \sum_{K \subset \omega_F} \mu_K h_K^2 \|\mathbf{f} - \mathbf{f}_h\|_{\mathbf{L}^2(K)}^2, \\ Ch_F \left\| \beta_F^{-1/2} \llbracket \beta \mathbf{u}_h \cdot \mathbf{n} \rrbracket_F \right\|_{\mathbf{L}^2(F)}^2 &\leq \|\beta^{1/2} (\mathbf{u} - \mathbf{u}_h)\|_{\mathbf{L}^2(\omega_F)}^2 + \sum_{K \subset \omega_F} \beta_K^{-1} h_K^2 \|\nabla \cdot \mathbf{f}\|_{\mathbf{L}^2(K)}^2, \\ \text{and } C \mu_K^{1/2} h_K \|\mathbf{f} - \beta \mathbf{u}_h - \nabla \times (\mu^{-1} \nabla \times \mathbf{u}_h)\|_{\mathbf{L}^2(K)} &\leq \|\mathbf{u} - \mathbf{u}_h\|_K, \end{aligned} \tag{4.15}$$

where the coefficients  $\mu_F^{-1}$  and  $\beta_F$  on face  $F$  are given by the arithmetic averages of  $\mu^{-1}$  and  $\beta$

$$\mu_F^{-1} = (\mu_{K_-}^{-1} + \mu_{K_+}^{-1})/2, \text{ and } \beta_F = (\beta_{K_-} + \beta_{K_+})/2,$$

respectively. Next we move on to prove the equivalence.

**Lemma 4.12** (Equivalence of  $\eta_{K,0}$ ). There exists a constant  $c > 0$  independent of the jumps of the coefficients such that for any  $K \in \mathcal{T}_h$ :

$$c \eta_{K,0} \leq \sum_{F \subset \partial K} h_F^{1/2} \left\| \beta_F^{-1/2} \llbracket \beta \mathbf{u}_h \cdot \mathbf{n} \rrbracket_F \right\|_{\mathbf{L}^2(F)}. \tag{4.16}$$

*Proof.* it suffices to show that  $\eta_{K,0}$  can be bounded by the summation of the residual-based estimator within the local face patch.

For any interior element  $K$ , we first use a partition of unity to bound the estimator  $\eta_{K,0}$  by the fact that  $\mathcal{ND}_0(K) \subset \mathbf{BDM}_1(K)$ . The difference of the weighted average  $\boldsymbol{\tau}_h^*$  and  $\boldsymbol{\tau}_h$  is

$$\begin{aligned} (\boldsymbol{\tau}_h^* - \boldsymbol{\tau}_h)|_K &= \sum_{F \subset \partial K \setminus \partial \Omega} \sum_{\mathbf{z} \in \mathcal{N}_h(F)} \left( \frac{1}{|F|} \int_F (\boldsymbol{\tau}_{h,F} - \boldsymbol{\tau}_{h,K}) \cdot \mathbf{n}_F \lambda_{\mathbf{z}} dS \right) \boldsymbol{\psi}_{F,\mathbf{z}} \\ &= \sum_{F \subset \partial K \setminus \partial \Omega} \sum_{\mathbf{z} \subset \mathcal{N}_h(F)} \frac{1 - \kappa_F^K}{|F|} \left( \int_F \llbracket \beta \mathbf{u}_h \cdot \mathbf{n} \rrbracket_F \lambda_{\mathbf{z}} dS \right) \boldsymbol{\psi}_{F,\mathbf{z}}. \end{aligned}$$

Recalling from (3.5) that on each face  $F$  of element  $K$ ,  $\kappa_F^K = \beta_K^{1/2} / (\beta_K^{1/2} + \beta_{K'}^{1/2})$ , where  $K'$  is the neighboring element sharing this fixed face  $F$  with  $K$ . Since

$$\|\lambda_{\mathbf{z}}\|_{\mathbf{L}^2(F)} \leq C |F|^{\frac{1}{2}} \quad \text{and} \quad \|\boldsymbol{\psi}_{F,\mathbf{z}}\|_{\mathbf{L}^2(K)} \leq C |K|^{\frac{1}{2}},$$

and using the following coefficient weight relation (3.5) on each face  $F$ :

$$(1 - \kappa_F^K) \beta_K^{-1/2} = \frac{1}{\beta_K^{1/2} + \beta_{K'}^{1/2}} \leq \frac{\sqrt{2}}{(\beta_K + \beta_{K'})^{1/2}} = \frac{1}{\beta_F^{1/2}},$$

the local error indicator  $\eta_{K,0}$  has the following bound:

$$\begin{aligned}
\eta_{K,0} &= \left\| \beta^{-1/2} \boldsymbol{\tau}_h^* - \beta^{1/2} \mathbf{u}_h \right\|_{\mathbf{L}^2(K)} = \left\| \beta^{-1/2} (\boldsymbol{\tau}_h^* - \boldsymbol{\tau}_h) \right\|_{\mathbf{L}^2(K)} \\
&\leq \sum_{F \subset \partial K \setminus \partial \Omega} \sum_{\mathbf{z} \subset \mathcal{N}_h(F)} \frac{1}{2|F|\beta_F^{1/2}} \left| \int_F [\![\beta \mathbf{u}_h \cdot \mathbf{n}]\!]_F \lambda_{\mathbf{z}} dS \right| \|\psi_{F,\mathbf{z}}\|_{\mathbf{L}^2(K)} \\
&\leq \sum_{F \subset \partial K \setminus \partial \Omega} C \left( \frac{|K|}{|F|} \right)^{1/2} \left\| \beta_F^{-1/2} [\![\beta \mathbf{u}_h \cdot \mathbf{n}]\!]_F \right\|_{L^2(F)}.
\end{aligned}$$

For any element with a boundary face, thanks to the setting for problem (2.15), that the Dirichlet data can be exactly represented by an  $\mathcal{ND}_0$  vector field's tangential trace, the degrees of freedom on any boundary face do not contribute to the approximation error in that element. This completes the proof of the lemma.  $\square$

**Lemma 4.13** (Equivalence of  $\eta_{K,\perp}$ ). Under Assumption 4.4, there exists a constant  $c > 0$  independent of the jumps of the coefficients such that for any  $K \in \mathcal{T}_h$

$$c \eta_{K,\perp} \leq \sum_{e \in \mathcal{E}_h(K)} \sum_{F \subset \omega_{e,F}} h_F^{1/2} \left\| \mu_F^{1/2} [\!(\mu^{-1} \nabla \times \mathbf{u}_h) \times \mathbf{n}]\!]_F \right\|_{\mathbf{L}^2(F)}. \quad (4.17)$$

*Proof.* The proof of this lemma uses the setting in the edge patch's illustration of Figure 1a. The edge patch  $\omega_e$  consists of 4 tetrahedra, and the following proof generalizes without essential changes to the case when there are more than 4 tetrahedra in  $\omega_e$ .

Without loss of generality, the element of interest  $K$  is assumed to be  $K_1$  in Figure 1a. First performing the partition of unity for  $\boldsymbol{\sigma}_{h,K} = \mu^{-1} \nabla \times \mathbf{u}_h|_K$ , which is a constant vector and can be represented by  $\mathcal{ND}_0(K)$  vector fields:

$$\begin{aligned}
\eta_{K,\perp} &= \left\| \mu^{\frac{1}{2}} \boldsymbol{\sigma}_h^* - \mu^{-\frac{1}{2}} \nabla \times \mathbf{u}_h \right\|_{\mathbf{L}^2(K)} = \left\| \mu^{\frac{1}{2}} \sum_{e \in \mathcal{E}_h(K)} (\boldsymbol{\sigma}_h^* - \boldsymbol{\sigma}_{h,K}) \cdot \mathbf{t}_e \boldsymbol{\varphi}_e \right\|_{\mathbf{L}^2(K)} \\
&\leq \sum_{e \in \mathcal{E}_h(K)} \left\| \mu^{\frac{1}{2}} (\boldsymbol{\sigma}_h^* - \boldsymbol{\sigma}_{h,K}) \cdot \mathbf{t}_e \boldsymbol{\varphi}_e \right\|_{\mathbf{L}^2(K)} \leq \sum_{e \in \mathcal{E}_h(K)} \mu_K^{\frac{1}{2}} |(\boldsymbol{\sigma}_h^* - \boldsymbol{\sigma}_{h,K}) \cdot \mathbf{t}_e| \|\boldsymbol{\varphi}_e\|_{\mathbf{L}^2(K)}.
\end{aligned} \quad (4.18)$$

By the fact that  $\|\boldsymbol{\varphi}_e\|_{\mathbf{L}^2(K)} \leq C|K|^{\frac{1}{2}}$ , the rest of the proof is to establish the equivalence, for every edge  $e$ , of  $|(\boldsymbol{\sigma}_h^* - \boldsymbol{\sigma}_{h,K}) \cdot \mathbf{t}_e|$  with the coefficient-weighted tangential jump term in the residual-based estimator.

For the rest of the proof let us assume the edge of interest is  $e$  in Figure 1a. Before moving on to different coefficient distribution scenarios in this edge patch,

first by the local recovery (3.7) and the  $\mathcal{ND}_0$  basis function construction (2.16), it is straightforward to check that

$$\boldsymbol{\sigma}_h^* \cdot \mathbf{t}_e = \frac{1}{|\widehat{\omega}_{e,F}|} \sum_{F \subset \widehat{\omega}_{e,F}} \int_F (\boldsymbol{\sigma}_{h,F} \cdot \mathbf{t}_e) dS.$$

The first case is when  $\widehat{\omega}_e = K = K_1$ , then  $\widehat{\omega}_{e,F} = F_1 \cup F_4$ . Using the geometric relation that for any  $\mathbf{v} \cdot \mathbf{t}_e = \mathbf{n}_F \times (\mathbf{v} \times \mathbf{n}_F) \cdot \mathbf{t}_e$  if  $\mathbf{t}_e$  lies on the planar surface  $F$ , and the definition of the weighted average  $\boldsymbol{\sigma}_{h,F_i}$  in (3.6), yields

$$\begin{aligned} (\boldsymbol{\sigma}_h^* - \boldsymbol{\sigma}_{h,K}) \cdot \mathbf{t}_e &= \frac{1}{|\widehat{\omega}_{e,F}|} \sum_{i \in \{1,4\}} \int_{F_i} (\boldsymbol{\sigma}_{h,F_i} - \boldsymbol{\sigma}_{h,K}) \cdot \mathbf{t}_e dS \\ &= \frac{1}{|\widehat{\omega}_{e,F}|} \sum_{i \in \{1,4\}} \int_{F_i} \mathbf{n}_{F_i} \times ((\boldsymbol{\sigma}_{h,F_i} - \boldsymbol{\sigma}_{h,K}) \times \mathbf{n}_{F_i}) \cdot \mathbf{t}_e dS \\ &= \frac{1}{|\widehat{\omega}_{e,F}|} \sum_{i \in \{1,4\}} \int_{F_i} (1 - \gamma_{F_i}^K) \llbracket (\mu^{-1} \nabla \times \mathbf{u}_h) \times \mathbf{n} \rrbracket_{F_i} \cdot (\mathbf{t}_e \times \mathbf{n}_{F_i}) dS. \end{aligned} \quad (4.19)$$

By the coefficient weight defined in (3.5), for  $F_1$  we have

$$\mu_K^{1/2} (1 - \gamma_{F_1}^K) = \frac{1}{\mu_K^{-1/2} + \mu_{K_2}^{-1/2}} \leq \frac{\sqrt{2}}{(\mu_K^{-1} + \mu_{K_2}^{-1})^{1/2}} = \mu_{F_1}^{1/2}.$$

By Cauchy-Schwarz inequality and the triangle inequality

$$\mu_K^{1/2} |(\boldsymbol{\sigma}_h^* - \boldsymbol{\sigma}_{h,K}) \cdot \mathbf{t}_e| \leq \frac{1}{2|\widehat{\omega}_{e,F}|} \sum_{i \in \{1,4\}} |F_i|^{1/2} \left\| \mu_{F_i}^{1/2} \llbracket (\mu^{-1} \nabla \times \mathbf{u}_h) \times \mathbf{n} \rrbracket_{F_i} \right\|_{L^2(F_i)}. \quad (4.20)$$

Then using the shape regularity of the mesh, i.e.  $|F_i|^{1/2} |K|^{1/2} |\widehat{\omega}_{e,F}|^{-1} \leq C h_{F_i}^{1/2}$  for any  $F_i$  in this edge patch, we have

$$\left\| \mu^{\frac{1}{2}} (\boldsymbol{\sigma}_h^* - \boldsymbol{\sigma}_{h,K}) \cdot \mathbf{t}_e \varphi_e \right\|_{L^2(K)} \leq \sum_{F \subset \widehat{\omega}_{e,F}} h_F^{1/2} \left\| \mu_F^{1/2} \llbracket (\mu^{-1} \nabla \times \mathbf{u}_h) \times \mathbf{n} \rrbracket_F \right\|_{L^2(F)}. \quad (4.21)$$

A variant of the first case is that  $K = K_1 \subsetneq \widehat{\omega}_{e,F}$ . Assume  $\widehat{\omega}_{e,F} = K_1 \cup K_2$ , then  $\widehat{\omega}_{e,F} = F_1 \cup F_2 \cup F_4$ . By the definition of  $\widehat{\omega}_{e,F}$  in (2.9),  $\mu_{K_1}^{-1} = \mu_{K_2}^{-1} = \min_{i=1,\dots,4} \mu_{K_i}^{-1}$ . The proof of the bound (4.20) for this variant shares almost the same argument with above, except there will be one extra term comparing to (4.19), and it can be

rewritten as follows:

$$\begin{aligned}
& \frac{1}{|\widehat{\omega}_{e,F}|} \int_{F_2} (\boldsymbol{\sigma}_{h,F_2} - \boldsymbol{\sigma}_{h,K}) \cdot \mathbf{t}_e \, dS \\
&= \frac{1}{|\widehat{\omega}_{e,F}|} \int_{F_2} \left[ (\boldsymbol{\sigma}_{h,F_2} - \boldsymbol{\sigma}_{h,K_2}) + (\boldsymbol{\sigma}_{h,K_2} - \boldsymbol{\sigma}_{h,K}) \right] \cdot \mathbf{t}_e \, dS \\
&= \frac{1}{|\widehat{\omega}_{e,F}|} \int_{F_2} (1 - \gamma_{F_2}^{K_2}) \llbracket (\mu^{-1} \nabla \times \mathbf{u}_h) \times \mathbf{n} \rrbracket_{F_2} \cdot (\mathbf{t}_e \times \mathbf{n}_{F_2}) \, dS \\
&\quad + \frac{1}{|\widehat{\omega}_{e,F}|} \int_{F_2} \llbracket (\mu^{-1} \nabla \times \mathbf{u}_h) \times \mathbf{n} \rrbracket_{F_1} \cdot (\mathbf{t}_e \times \mathbf{n}_{F_1}) \, dS.
\end{aligned} \tag{4.22}$$

Using the shape regularity of the edge patch ( $c|F_2| \leq |F_1| \leq C|F_2|$ ), and the fact that

$$\mu_K^{1/2} (1 - \gamma_{F_2}^{K_2}) = \mu_{K_2}^{1/2} (1 - \gamma_{F_2}^{K_2}) \leq \mu_{F_2}^{1/2}, \quad \text{and} \quad \mu_K^{1/2} = \frac{2}{\mu_K^{-1/2} + \mu_{K_2}^{-1/2}} \leq 2\mu_{F_1}^{1/2},$$

we reach the following estimate

$$\begin{aligned}
& \mu_K^{1/2} \left| \frac{1}{|\widehat{\omega}_{e,F}|} \int_{F_2} (\boldsymbol{\sigma}_{h,F_2} - \boldsymbol{\sigma}_{h,K}) \cdot \mathbf{t}_e \, dS \right| \\
& \leq \frac{C}{|\widehat{\omega}_{e,F}|} \sum_{i \in \{1, 2\}} |F_i|^{1/2} \left\| \mu_{F_i}^{1/2} \llbracket (\mu^{-1} \nabla \times \mathbf{u}_h) \times \mathbf{n} \rrbracket_{F_i} \right\|_{L^2(F_i)}.
\end{aligned} \tag{4.23}$$

Thus the estimate (4.21) follows. If  $\widehat{\omega}_e$  contains more elements, the same argument with above applies, with all the unweighted extra terms involve only the interior faces of  $\widehat{\omega}_e$ . This completes the proof for the first case.

The second case when  $K = K_1 \not\subset \widehat{\omega}_e$ , yet  $K$  is adjacent to  $\widehat{\omega}_e$ . Assume  $K_2 = \widehat{\omega}_e$ , i.e.,  $\widehat{\omega}_{e,F} = F_1 \cup F_2$ . A similar split as (4.19) applies

$$(\boldsymbol{\sigma}_h^* - \boldsymbol{\sigma}_{h,K}) \cdot \mathbf{t}_e = \frac{1}{|\widehat{\omega}_{e,F}|} \sum_{i \in \{1, 2\}} \int_{F_i} (\boldsymbol{\sigma}_{h,F_i} - \boldsymbol{\sigma}_{h,K}) \cdot \mathbf{t}_e \, dS.$$

The  $F_1$  term can be estimated the same with (4.20). The  $F_2$  term can be rewritten as (4.22). This time we use  $\mu_K^{-1} \geq \mu_{K_2}^{-1} = \min_{i=1, \dots, 4} \mu_{K_i}^{-1}$ , this implies

$$\mu_K^{1/2} \leq \frac{2}{\mu_K^{-1/2} + \mu_{K_2}^{-1/2}} \leq 2\mu_{F_1}^{1/2},$$

thus the estimate (4.23) follows, which, under some backtracking, confirms the validities of estimates (4.20) and (4.21). If  $\widehat{\omega}_e$  contains more elements than  $K_2$ , same argument applies as long as  $\mu_K^{-1} \geq \mu_{\widehat{\omega}_e}^{-1}$  and the shape regularity holds for the edge patch of interest. This completes the proof for the second case.

The third case is that  $K = K_1 \not\subset \widehat{\omega}_e$ , nor is  $K$  neighboring to  $\widehat{\omega}_e$ . Assuming  $\widehat{\omega}_e = K_3$ , then  $\widehat{\omega}_{e,F} = F_2 \cup F_3$ . The same split with (4.19) applies, but this time on face  $F_2$  and  $F_3$ ,

$$(\boldsymbol{\sigma}_h^* - \boldsymbol{\sigma}_{h,K}) \cdot \mathbf{t}_e = \frac{1}{|\widehat{\omega}_{e,F}|} \sum_{i \in \{2,3\}} \int_{F_i} (\boldsymbol{\sigma}_{h,F_i} - \boldsymbol{\sigma}_{h,K}) \cdot \mathbf{t}_e \, dS.$$

In this lemma, Assumption 4.4 holds. Without loss of generality, we assume the monotone path from  $K = K_1$  to  $K_3$  is through  $K_2$ . The  $F_2$  term can be estimated exactly like previous case, because  $\mu_K^{-1} \geq \mu_{K_2}^{-1} \geq \mu_{K_3}^{-1} = \min_{i=1,\dots,4} \mu_{K_i}^{-1}$ . For the  $F_3$  term, using the same trick as (4.22) yields:

$$\begin{aligned} & \frac{1}{|\widehat{\omega}_{e,F}|} \int_{F_3} (\boldsymbol{\sigma}_{h,F_3} - \boldsymbol{\sigma}_{h,K}) \cdot \mathbf{t}_e \, dS \\ &= \frac{1}{|\widehat{\omega}_{e,F}|} \int_{F_3} [(\boldsymbol{\sigma}_{h,F_3} - \boldsymbol{\sigma}_{h,K_3}) + (\boldsymbol{\sigma}_{h,K_3} - \boldsymbol{\sigma}_{h,K_2}) + (\boldsymbol{\sigma}_{h,K_2} - \boldsymbol{\sigma}_{h,K})] \cdot \mathbf{t}_e \, dS \\ &= \frac{1}{|\widehat{\omega}_{e,F}|} \int_{F_3} (1 - \gamma_{F_3}^{K_3}) \llbracket (\mu^{-1} \nabla \times \mathbf{u}_h) \times \mathbf{n} \rrbracket_{F_3} \cdot (\mathbf{t}_e \times \mathbf{n}_{F_3}) \, dS \\ & \quad + \frac{1}{|\widehat{\omega}_{e,F}|} \sum_{i \in \{1,2\}} \int_{F_3} \llbracket (\mu^{-1} \nabla \times \mathbf{u}_h) \times \mathbf{n} \rrbracket_{F_i} \cdot (\mathbf{t}_e \times \mathbf{n}_{F_i}) \, dS. \end{aligned}$$

By the quasi-monotonicity of the coefficient on this edge patch again, we have

$$\mu_K^{1/2} (1 - \gamma_{F_3}^{K_3}) \leq \mu_{K_3}^{1/2} (1 - \gamma_{F_3}^{K_3}) \leq \mu_{F_3}^{1/2}, \quad \text{and} \quad \mu_K^{1/2} \leq \frac{2}{\mu_{K_2}^{-1/2} + \mu_{K_3}^{-1/2}} \leq 2\mu_{F_2}^{1/2},$$

therefore, the estimate for the  $F_3$  term is similar to (4.23), with one extra face included due to the fact that the inequality is passed through an intermediate element along the monotone path

$$\begin{aligned} & \mu_K^{1/2} \left| \frac{1}{|\widehat{\omega}_{e,F}|} \int_{F_3} (\boldsymbol{\sigma}_{h,F_3} - \boldsymbol{\sigma}_{h,K}) \cdot \mathbf{t}_e \, dS \right| \\ & \leq \frac{C}{|\widehat{\omega}_{e,F}|} \sum_{i \in \{1,2,3\}} |F_i|^{1/2} \left\| \mu_{F_i}^{1/2} \llbracket (\mu^{-1} \nabla \times \mathbf{u}_h) \times \mathbf{n} \rrbracket_{F_i} \right\|_{\mathbf{L}^2(F_i)}. \end{aligned} \tag{4.24}$$

Consequently, estimates (4.20) and (4.21) follow for the third case. If the reader walks through the proof, one will find that more tetrahedra being contained in  $\widehat{\omega}_e$  than 1 does not change the essential part of the proof because of the existence of the monotone path. This completes the proof of the lemma.  $\square$

**Theorem 4.14** (Local Efficiency of  $\eta_K$ ). *Under Assumption 4.4, there exists a constant  $c > 0$  independent of the jumps of the coefficients such that for any  $K \in \mathcal{T}_h$ :*

$$c \eta_K \leq \|\mathbf{u} - \mathbf{u}_h\|_{\omega_{K,F}} + \text{osc}(\mathbf{f}, \mu, \beta; \omega_{K,F}), \tag{4.25}$$

where  $\text{osc}(\mathbf{f}, \mu, \beta; \omega_{K,F})$  is the oscillation of the data within  $\omega_{K,F}$

$$\text{osc}(\mathbf{f}, \mu, \beta; \omega_{K,F}) = \left\{ \sum_{K \subset \omega_{K,F}} \left( \beta_K^{-1} h_K^2 \|\nabla \cdot \mathbf{f}\|_{L^2(K)}^2 + \mu_K h_K^2 \|\mathbf{f} - \mathbf{f}_h\|_{L^2(K)}^2 \right) \right\}^{1/2}.$$

*Proof.* By the residual-based estimator local efficiency estimate (4.15), Lemma 4.12 and 4.13 which show the recovery-based  $\eta_{K,0}$  and  $\eta_{K,\perp}$  can be bounded the face jumps in the residual-based estimator, it suffices to show that the local recovery-based residual term is locally efficient. Applying the triangle inequality for  $\eta_{K,R}$  gives:

$$\eta_{K,R} \leq \mu_K^{1/2} h_K \left( \|\mathbf{f} - \beta \mathbf{u}_h - \nabla \times (\mu^{-1} \nabla \times \mathbf{u}_h)\|_{L^2(K)} + \|\nabla \times (\mu^{-1} \nabla \times \mathbf{u}_h - \boldsymbol{\sigma}_h^*)\|_{L^2(K)} \right),$$

which, together with a standard inverse inequality and (4.15), shows that

$$c \eta_{K,R} \leq \|\mathbf{u} - \mathbf{u}_h\|_K + \eta_{K,\perp}.$$

This completes the proof of the theorem.  $\square$

## 5 Numerical Experiments

This section reports numerical results of our estimator on several three dimensional  $\mathbf{H}(\text{curl})$  interface test problems.

The numerical tests are implemented under *iFEM* (see [11]) framework in MATLAB. Initial meshes are generated by the MATLAB built-in `DelaunayTri` and `distmesh` (see [32]). At each iteration, let  $\mathcal{S}_h$  be a subset of  $\mathcal{T}_h$  whose elements satisfy

$$\sum_{K \in \mathcal{S}_h} \eta_K^2 \geq \theta \sum_{K \in \mathcal{T}_h} \eta_K^2,$$

where the  $\eta_K$  is evaluated using the recovered quantities computed by weighted  $\mathbf{L}^2$ -projections through multigrid  $V(3, 2)$ -cycle iterations. This procedure is analyzed in [39] for diffusion problem, and is proved to be equivalent to the local weighted averaging. The marking parameter  $\theta$  is chosen to be 0.2. All elements in  $\mathcal{S}_h$  are refined locally by bisecting the longest edge, and some neighboring elements of  $\mathcal{S}_h$  are refined to preserve conformity of the triangulation.

To measure the global reliability of the *a posteriori* error estimator, we show comparisons of different measures in the each example's table of comparison.  $n$  is the number of levels of refinement. The  $N_n$  the dimension of  $\mathcal{E}_{h,n}$  in the  $n$ -th level triangulation, in our case, it is the number of degrees of freedom. The *effectivity index* for each estimator at the  $n$ -th level is:

$$\text{eff-index} := \frac{\eta_n}{\|\mathbf{u} - \mathbf{u}_{h,n}\|},$$

where  $\eta_n$  is the error estimator, and  $\mathbf{u}_{h,n}$  is the finite element approximation at the  $n$ -th level of triangulation.

The *orders of convergence* are computed for both  $\eta$  and  $\|\mathbf{u} - \mathbf{u}_h\|$ .  $r_\eta$  and  $r_{\text{err}}$  are defined as the slope for the line of  $\eta_n$  and  $\|\mathbf{u} - \mathbf{u}_{h,n}\|$  in the log-log scale plot, such that

$$\ln \eta_n \sim -r_\eta \ln N_n + c_1, \quad \text{and} \quad \ln \|\mathbf{u} - \mathbf{u}_{h,n}\| \sim -r_{\text{err}} \ln N_n + c_2.$$

In the convergence rate plot, the log of degrees of freedom is the horizontal axis, and the log of the error/estimator is the vertical axis. The order of convergence is optimal when  $r_\eta$  and  $r_{\text{err}}$  are approximately 1/3.

In first two examples with known true solutions, the adaptive mesh refinement procedure is terminated when the true relative error

$$\text{rel-error} := \|\mathbf{u} - \mathbf{u}_h\| / \|\mathbf{u}\| \leq \text{Tol}.$$

For comparison, numerical results involve some of the following error estimators other than the recovery estimator in (3.8):

1. The residual estimator in [3]:

$$\begin{aligned} \eta_{K,Res}^2 &= \mu_K h_K^2 \|\mathbf{f} - \beta \mathbf{u}_h - \nabla \times (\mu^{-1} \nabla \times \mathbf{u}_h)\|_{\mathbf{L}^2(K)}^2 + \beta_K^{-1} h_K^2 \|\nabla \cdot (\beta \mathbf{u}_h - \mathbf{f})\|_{\mathbf{L}^2(K)}^2 \\ &+ \sum_{F \in \mathcal{F}_h(K)} \frac{h_F}{2} \left( \beta_F^{-1} \|\llbracket \beta \mathbf{u}_h \cdot \mathbf{n}_F \rrbracket\|_{L^2(F)}^2 + \mu_F \|\llbracket (\mu^{-1} \nabla \times \mathbf{u}_h) \times \mathbf{n} \rrbracket\|_{L^2(F)}^2 \right), \end{aligned} \quad (5.1)$$

and  $\eta_{Res}^2 = \sum_{K \in \mathcal{T}_h} \eta_{K,Res}^2$ , where  $\mu_F^{-1}$  and  $\beta_F$  are the arithmetic averages of  $\mu^{-1}$  and  $\beta$ , respectively, on elements sharing the face  $F$ . Note that this estimator is weighted appropriately and may be viewed as the extension of the residual estimator in [4, 33] for the diffusion interface problem to the  $\mathbf{H}(\text{curl})$  interface problem.

2. The Zienkiewicz-Zhu (ZZ) based error estimator in [30] using the coefficient-weighted norm (2.4):

$$\begin{aligned} \eta_{K,ZZ}^2 &= \left\| \mu^{-1/2} \mathcal{R}_\perp(\nabla \times \mathbf{u}_h) - \mu^{-1/2} \nabla \times \mathbf{u}_h \right\|_{\mathbf{L}^2(K)}^2 \\ &+ \left\| \beta^{1/2} \mathcal{R}_0(\mathbf{u}_h) - \beta^{1/2} \mathbf{u}_h \right\|_{\mathbf{L}^2(K)}^2, \end{aligned} \quad (5.2)$$

and  $\eta_{ZZ}^2 = \sum_{K \in \mathcal{T}_h} \eta_{K,ZZ}^2$ . Both recovered quantities  $\mathcal{R}_\perp(\nabla \times \mathbf{u}_h)$  and  $\mathcal{R}_0(\mathbf{u}_h)$  are in the continuous piecewise linear vector fields space  $\mathcal{P}_1 := \{\mathbf{p} \in \mathbf{H}^1(\Omega) : \mathbf{p}|_K \in \mathbf{P}_1(K)\}$ , and their nodal values at any vertex  $\mathbf{z} \in \mathcal{N}_h$  are:

$$\mathcal{R}_\perp(\nabla \times \mathbf{u}_h)|_{\mathbf{z}} = \frac{1}{|\omega_{\mathbf{z}}|} \int_{\omega_{\mathbf{z}}} \nabla \times \mathbf{u}_h \, d\mathbf{x} \quad \text{and} \quad \mathcal{R}_0(\mathbf{u}_h)|_{\mathbf{z}} = \frac{1}{|\omega_{\mathbf{z}}|} \int_{\omega_{\mathbf{z}}} \mathbf{u}_h \, d\mathbf{x}.$$

3. The Zienkiewicz-Zhu (ZZ) flux based error estimator in [30] with weight suited to the coefficient-weighted norm (2.4):

$$\begin{aligned}\eta_{K,ZZ,f}^2 &= \left\| \mu^{1/2} \mathcal{R}_\perp(\mu^{-1} \nabla \times \mathbf{u}_h) - \mu^{-1/2} \nabla \times \mathbf{u}_h \right\|_{\mathbf{L}^2(K)}^2 \\ &\quad + \left\| \beta^{-1/2} \mathcal{R}_0(\beta \mathbf{u}_h) - \beta^{1/2} \mathbf{u}_h \right\|_{\mathbf{L}^2(K)}^2\end{aligned}\quad (5.3)$$

and  $\eta_{ZZ,f}^2 = \sum_{K \in \mathcal{T}_h} \eta_{K,ZZ,f}^2$ . Both recovered quantities  $\mathcal{R}_\perp(\mu^{-1} \nabla \times \mathbf{u}_h)$  and  $\mathcal{R}_0(\beta \mathbf{u}_h)$  are in  $\mathcal{P}_1$  as well, and their nodal values at any vertex  $\mathbf{z} \in \mathcal{N}_h$  are:

$$\mathcal{R}_\perp(\mu^{-1} \nabla \times \mathbf{u}_h)|_{\mathbf{z}} = \frac{1}{|\omega_{\mathbf{z}}|} \int_{\omega_{\mathbf{z}}} \mu^{-1} \nabla \times \mathbf{u}_h \, d\mathbf{x} \quad \text{and} \quad \mathcal{R}_0(\beta \mathbf{u}_h)|_{\mathbf{z}} = \frac{1}{|\omega_{\mathbf{z}}|} \int_{\omega_{\mathbf{z}}} \beta \mathbf{u}_h \, d\mathbf{x}.$$

**Example 1:** This example is adapted from a benchmark test problem (see [7, 8, 26]) for elliptic interface problems. The computational domain is a narrow slit along  $z$ -direction:  $\Omega = (-1, 1)^2 \times (-\delta, \delta)$  with  $\delta = 0.2$ . The true solution  $\mathbf{u}$  is given in cylindrical coordinates  $(r, \theta, z)$ :

$$\mathbf{u} = \nabla \psi = \nabla(r^\alpha \phi(\theta)),$$

where  $\phi(\theta)$  takes different values within four different subdomains while being glued together using continuity conditions that is firstly invented in [26]. The  $\mu = 1$ , and the  $\beta$  is given by

$$\beta = \begin{cases} R & \text{in } (0, 1)^2 \times (-\delta, \delta) \cup (1, 0)^2 \times (-\delta, \delta), \\ 1 & \text{in } \Omega \setminus \left( (0, 1)^2 \times (-\delta, \delta) \cup (1, 0)^2 \times (-\delta, \delta) \right). \end{cases}$$

Here we set parameters  $\alpha, R$  to be

$$\alpha = 0.5, \quad R \approx 5.8284271247461907.$$

In this example, The tolerance is set to be  $\text{Tol} = 0.1$ . The numerical results of example 1 are in Table 1. It shows that to achieve approximately the same level of relative error, the number of degrees of freedom needed in the mesh refined by the local indicator  $\eta_{K,ZZ}$  or  $\eta_{K,ZZ,f}$  requires more than twice than the other two.

The adaptively refined mesh generated by each estimator can be found in Figure 5. The tendency of  $\eta_{ZZ}$  or  $\eta_{ZZ,f}$  to over-refine those four interfaces is due to the fact that recovered quantities enforce unnecessary extra continuity conditions of the true quantities. For example,  $\mathcal{R}_\perp(\mu^{-1} \nabla \times \mathbf{u}_h)$  and  $\mathcal{R}_0(\beta \mathbf{u}_h)$  in (5.3) are in  $\mathbf{H}^1(\Omega)$ , yet for the true solution  $\mathbf{u}$ ,  $\mu^{-1} \nabla \times \mathbf{u} \in \mathbf{H}(\mathbf{curl}; \Omega)$  and  $\beta \mathbf{u} \in \mathbf{H}(\mathbf{div}; \Omega)$  in (3.4).

Overall, the recovery-based error estimator and residual-based error estimator lead to the correctly refined mesh, and the recovery-based one performs more convincingly showing a less oscillatory convergence, achieving the same level of relative error in fewer iterations. More importantly, it exhibits a better effectivity index.

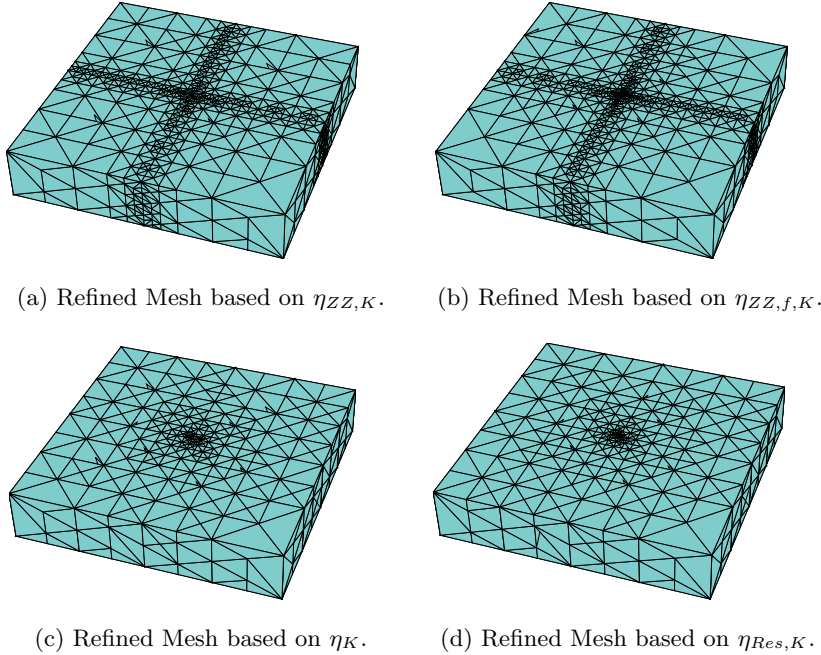


Figure 5: Mesh Result of Example 1

Table 1: Comparison of the estimators in Example 1

	$n$	# DoF	rel-error	eff-index	$r_\eta$	$r_{\text{err}}$
$\eta_{ZZ}$	30	39391	0.0898	1.309	0.128	0.235
$\eta_{ZZ,f}$	26	44111	0.0837	1.495	0.243	0.253
$\eta_{Res}$	24	18832	0.0873	1.749	0.257	0.301
$\eta$	18	18649	0.0886	0.820	0.299	0.303

**Example 2:** This example is in the numerical experiments section of [24]. The domain is  $\Omega = B_2 = \{(x, y, z) : x^2 + y^2 + z^2 < 2\}$ , and the coefficients are given by

$$\begin{cases} \mu = \mu_1 = 1, \beta = 1 & \text{in } B_1 = \{(x, y, z) : x^2 + y^2 + z^2 < 1\}, \\ \mu = \mu_2 = 10^6, \beta = 1 & \text{in } \Omega \setminus B_1. \end{cases}$$

The true solution  $\mathbf{u}$  is given by  $\mu \mathbf{u}_1$  in  $B_1$ , and  $\mu \mathbf{u}_2$  in  $\Omega \setminus B_1$ . For the explicit expression please refer to [24]. The  $\text{Tol} = 0.2$  in this example.

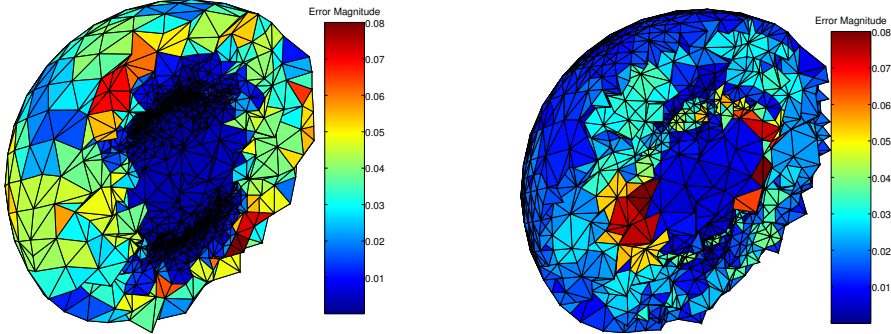
In this example, the element residual term  $\eta_R$  in (3.8) is not a higher order term (see Figure 7a). The red dashed line is a reference line of a constant multiple of  $(\# \text{DoF})^{-1/3}$ . The numerical results of example 2 are in Table 2. The adaptively refined mesh of each estimator can be found in Figure 6.

The refined meshes based on  $\eta_{K,Res}$ , and  $\eta_K$  respectively are visually similar, the

$\eta_{K,ZZ}$  and  $\eta_{K,ZZ,f}$  tend to over-refine the region where the local coefficient-weighted error is not significant yet  $\mu^{-1}\nabla \times \mathbf{u}$  is discontinuous across the interface.

Table 2: Comparison of the estimators in Example 2

	$n$	# DoF	rel-error	eff-index	$r_\eta$	$r_{\text{err}}$
$\eta_{ZZ}$	18	200692	0.199	4.077	Not converging	0.118
$\eta_{ZZ,f}$	20	99794	0.193	2.527	0.839	0.169
$\eta_{\text{Res}}$	9	63405	0.186	1.761	0.273	0.236
$\eta$	8	52287	0.193	1.079	0.282	0.251



(a) Relative error distribution of refined mesh based on  $\eta_{K,ZZ,f}$  cut on  $y = 0$ , it can be observed that the local errors are not evenly distributed. (b) Relative error distribution of refined mesh based on  $\eta_K$  cut on  $y = 0$ , the local errors are more evenly distributed than the mesh refined based on  $\eta_{K,ZZ,f}$ .

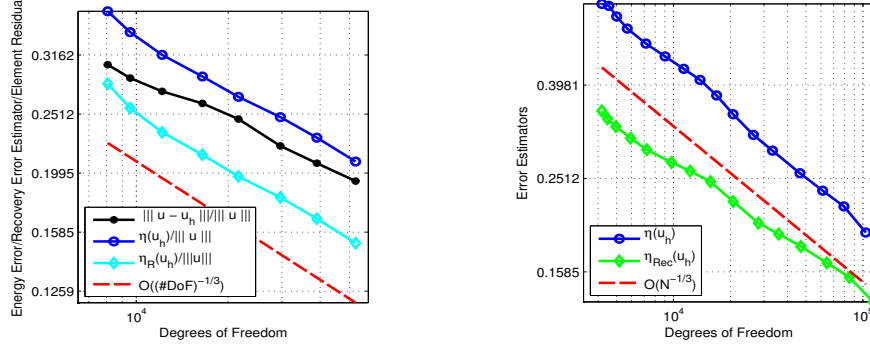
Figure 6: Relative error distributions result of Example 2

**Example 3:** This example is a widely-used test problem examining the performance of adaptive mesh refinement procedure for Maxwell equations (e.g. see [23]). The true solution is unknown and not smooth. The homogeneous Dirichlet boundary condition is enforced, together with a constant source current  $\mathbf{f} = (1, 1, 1)$ . The coefficients are given by:

$$\begin{cases} \mu = 1, \beta = 1 & \text{in } \Omega_c, \\ \mu = 1, \beta = 100 & \text{in } \Omega \setminus \Omega_c \end{cases}$$

where  $\Omega_c$  is  $\{(x, y, z) : |x|, |y|, |z| \leq \frac{1}{2}\}$ . In this example, we can not compute the true error, hence we set the stop criterion to be  $\eta \leq \text{Tol}$  with  $\text{Tol} = 0.16$  at the  $n$ -th level of triangulation.

This example illustrates two important aspects: (1) the element residual is indispensable in the error estimator in the pre-asymptotic region; (2) the iterative refining procedure using the residual-based estimator engages much more degrees of



(a) Example 2: convergence of  $\eta$ , comparing to the element residual term  $\eta_R$ . (b) Example 3: convergence of  $\eta$  versus the recovery-based only  $\eta_{Rec} = (\eta_{\perp}^2 + \eta_0^2)^{1/2}$ .

Figure 7: Convergence Results of Example 2 and Example 3

Table 3: Comparison of the estimators in Example 3

	$n$	#(DoF)	Estimator	$r_\eta$
$\eta_{Res}$	21	219993	0.156	0.328
$\eta$	14	61302	0.152	0.346
$\eta_{Rec}$	8	15672	0.159	0.230

freedom than the one using the recovery-based estimator, when same stop criterion is used for both.

The recovery-based error estimator shows an optimal order of convergence, which is  $\eta \sim (\#DoF)^{-1/3}$ , i.e.,  $r_\eta \approx 1/3$ , if the local error indicator includes the element residual  $\eta_K := (\eta_{K,\perp}^2 + \eta_{K,0}^2 + \eta_{K,R}^2)^{1/2}$ . If the element residual is discarded, i.e., the pure recovery-based estimator  $\eta_{K,Rec} := (\eta_{K,\perp}^2 + \eta_{K,0}^2)^{1/2}$  is used as the local error indicator, the order of convergence for  $\eta_{Rec} := \left( \sum_{K \in \mathcal{T}_h} \eta_{K,Rec}^2 \right)^{1/2}$  is not optimal (see Figure 7b, and Table 3).

From the first two examples, we learn that the effectivity index of the recovery-based estimator is in general two times as effective as that of the residual-based estimator. For problem with an unknown solution which is quite common originated from some real world applications, when setting the stopping criterion using the global error estimator, the number of degrees of freedom using the residual-based error estimator is  $(\text{eff-index}_{\text{Res}}/\text{eff-index}_{\text{Rec}})^3$  as much as that using the recovery-based error estimator (see Table 3).

## A Weighted Helmholtz Decomposition

Here we establish a weighted Helmholtz decomposition in light of [17, 18] tailored for the  $\mathbf{H}(\mathbf{curl})$  interface problem. The following assumption is needed to guarantee that such a decomposition exists with the constant in estimate (4.13) is independent of the jumps of the coefficients. In other words, the constant in the estimate depends on the jump size of the product of two coefficients, and the geometries of the interfaces as well.

**Assumption A.1.** (i) *The domain  $\Omega$  is assumed to be convex, simply-connected, and that no three or more subdomains share one edge from the triangulation of  $\Omega$ .*  
(ii) *The coefficients  $\mu$  and  $\beta$  are assumed to satisfy:  $C_{\min} \leq \mu_j \beta_j \leq C_{\max}$ , where  $C_{\min}$  and  $C_{\max}$  are two constants independent of the jumps of  $\mu_j$  and  $\beta_j$ , or  $\Omega_j$  on each subdomain  $\Omega_j$ .*

Firstly, we define some additional function spaces, along with the  $\mathbf{X}(\Omega, \beta)$  in (4.1), relevant to the weighted Helmholtz decomposition as follows: for any piecewise constant  $\alpha = \alpha_j$  in  $\Omega_j$ :

$$\begin{aligned}\mathring{\mathbf{H}}_0(\mathbf{curl}; \Omega) &= \{\mathbf{u} \in \mathbf{H}_0(\mathbf{curl}; \Omega) : \nabla \times \mathbf{u} = 0 \text{ in } \Omega\}, \\ PC^\infty(\Omega, \mathcal{P}) &= \{\mathbf{v} \in \mathbf{L}^2(\Omega) : \mathbf{v}|_{\Omega_j} \in \mathbf{C}^\infty(\Omega_j), j = 1, \dots, m\}, \\ \text{and } PH^s(\Omega, \mathcal{P}) &= \{v \in L^2(\Omega) : v|_{\Omega_j} \in H^s(\Omega_j), j = 1, \dots, m\}.\end{aligned}\quad (\text{A.1})$$

It is well known (see [21]) that the kernel of curl operator,  $\mathring{\mathbf{H}}_0(\mathbf{curl}; \Omega)$ , is characterized by the gradient field in a simply-connected domain:

**Lemma A.2.** If  $\Omega$  is simply-connected, for any  $\mathbf{u} \in \mathring{\mathbf{H}}_0(\mathbf{curl}; \Omega)$ , there exists a unique function  $\psi \in H_0^1(\Omega)$  such that  $\mathbf{u} = \nabla \psi$ .

Since  $\mathcal{A}(\mathbf{v}, \nabla \psi) = (\beta \mathbf{v}, \nabla \psi)$ , the orthogonal complement of  $\mathring{\mathbf{H}}_0(\mathbf{curl}; \Omega) = \nabla H_0^1(\Omega)$  with respect to  $\mathcal{A}(\cdot, \cdot)$  is

$$\{\mathbf{v} \in \mathbf{H}_0(\mathbf{curl}; \Omega) : (\beta \mathbf{v}, \nabla \psi) = 0 \ \forall \psi \in H_0^1(\Omega)\} \subset \mathbf{X}(\Omega, \beta).$$

To construct a weighted Helmholtz decomposition tailored for the interface problem, an analysis of the structure of  $\mathbf{X}(\Omega, \beta)$  is necessary. Before tackling this, the following lemma from [18] is needed:

**Lemma A.3.**  $\mathbf{X}(\Omega, \alpha) \cap PC^\infty(\Omega, \mathcal{P})$  is dense in  $\mathbf{X}(\Omega, \alpha) \cap PH^1(\Omega, \mathcal{P})$  in the following norm:

$$\|\mathbf{v}\|_{\mathbf{X}(\Omega)}^2 = \|\mathbf{v}\|_{\mathbf{L}^2(\Omega)}^2 + \|\nabla \times \mathbf{v}\|_{\mathbf{L}^2(\Omega)}^2 + \|\nabla \cdot (\alpha \mathbf{v})\|_{L^2(\Omega)}^2.$$

Now we move on to prove the norm equivalence for certain piecewise  $\mathbf{H}^1$ -vector fields using the density argument of Lemma A.3.

**Lemma A.4** (Norm equivalence for piecewise smooth vector fields). For all  $\mathbf{v} \in \mathbf{X}(\Omega, \alpha) \cap PH^1(\Omega, \mathcal{P})$ , the following identity holds:

$$\sum_{j=1}^m \int_{\Omega_j} \alpha |\nabla \mathbf{v}|^2 = \int_{\Omega} (\alpha |\nabla \times \mathbf{v}|^2 + \alpha^{-1} |\nabla \cdot (\alpha \mathbf{v})|^2). \quad (\text{A.2})$$

*Proof.* By Lemma A.3, it suffices to establish identity (A.2) for any  $\phi \in \mathbf{X}(\Omega, \alpha) \cap PC^\infty(\Omega, \mathcal{P})$ . To this end, using a local identity  $-\Delta \phi = \nabla \times (\nabla \times \phi) - \nabla (\nabla \cdot \phi)$  and integrating by parts on each subdomain  $\Omega_j$  twice give:

$$\begin{aligned} \sum_{j=1}^m \int_{\Omega_j} \alpha |\nabla \phi|^2 &= \sum_{j=1}^m \int_{\Omega_j} \alpha_j (|\nabla \times \phi|^2 + |\nabla \cdot \phi|^2) + B \\ \text{with } B &= \sum_{j=1}^m \int_{\partial \Omega_j} \alpha_j \left( (\mathbf{n} \cdot \nabla) \phi + \mathbf{n} \times (\nabla \times \phi) - (\nabla \cdot \phi) \mathbf{n} \right) \cdot \phi \, dS. \end{aligned}$$

Now, it remains to prove that  $B = 0$ . On any polygonal face with normal vector  $\mathbf{n}$  that is represented by the cartesian coordinates in the three dimensional space, rather than the local planar coordinates,  $\phi$  may be decomposed into the normal and tangential components as follows:

$$\phi = (\phi \cdot \mathbf{n}) \mathbf{n} + \phi_{\top} \quad \text{with } \phi_{\top} = \mathbf{n} \times (\phi \times \mathbf{n}), \quad (\text{A.3})$$

which, in turn, implies

$$\begin{aligned} (\mathbf{n} \cdot \nabla) \phi &= ((\mathbf{n} \cdot \nabla)(\phi \cdot \mathbf{n})) \mathbf{n} + (\mathbf{n} \cdot \nabla) \phi_{\top} \\ \text{and } \nabla \cdot \phi &= \nabla \cdot ((\phi \cdot \mathbf{n}) \mathbf{n}) + \nabla \cdot \phi_{\top} = (\mathbf{n} \cdot \nabla)(\phi \cdot \mathbf{n}) + \nabla \cdot \phi_{\top}. \end{aligned} \quad (\text{A.4})$$

By using the following identity (e.g. see [2])

$$\nabla(\mathbf{a} \cdot \mathbf{b}) = (\mathbf{a} \cdot \nabla) \mathbf{b} + (\mathbf{b} \cdot \nabla) \mathbf{a} + \mathbf{a} \times (\nabla \times \mathbf{b}) + \mathbf{b} \times (\nabla \times \mathbf{a})$$

and noticing that  $\mathbf{n}$  is a constant vector on a face, we have

$$\nabla(\mathbf{n} \cdot \phi) = (\mathbf{n} \cdot \nabla) \phi + \mathbf{n} \times (\nabla \times \phi),$$

which yields the following by being projected onto each polygonal face

$$\nabla_{\top}(\mathbf{n} \cdot \phi) = (\mathbf{n} \cdot \nabla) \phi_{\top} + \mathbf{n} \times (\nabla \times \phi), \quad (\text{A.5})$$

where  $\nabla_{\top}$  is defined as  $\nabla_{\top} u = (\nabla u)_{\top}$ . It follows from (A.4), (A.5), (A.3), homo-

geneous boundary condition, and identity (2.7) that:

$$\begin{aligned}
B &= \sum_{j=1}^m \int_{\partial\Omega_j} \alpha_j \left( \nabla_{\top}(\mathbf{n} \cdot \boldsymbol{\phi}) - (\nabla \cdot \boldsymbol{\phi}_{\top}) \mathbf{n} \right) \cdot \boldsymbol{\phi} \, dS \\
&= \sum_{j=1}^m \int_{\partial\Omega_j} \alpha_j \left( \nabla_{\top}(\mathbf{n} \cdot \boldsymbol{\phi}) \cdot \boldsymbol{\phi}_{\top} - (\nabla \cdot \boldsymbol{\phi}_{\top})(\boldsymbol{\phi} \cdot \mathbf{n}) \right) \, dS \\
&= \sum_{F \subset \mathfrak{I}} \int_F \left( [\![\nabla_{\top}(\alpha \boldsymbol{\phi} \cdot \mathbf{n}) \cdot \boldsymbol{\phi}_{\top}]\!]_F - [\![(\nabla \cdot \boldsymbol{\phi}_{\top})(\alpha \boldsymbol{\phi} \cdot \mathbf{n})]\!]_F \right) \, dS \\
&= \sum_{F \subset \mathfrak{I}} \int_F \left( \nabla_{\top}([\![\alpha \boldsymbol{\phi} \cdot \mathbf{n}]\!]_F) \cdot \boldsymbol{\phi}_{\top} + \nabla \cdot [\![\boldsymbol{\phi}_{\top}]\!]_F (\alpha \boldsymbol{\phi} \cdot \mathbf{n}) \right. \\
&\quad \left. + \nabla_{\top}(\alpha \boldsymbol{\phi} \cdot \mathbf{n}) \cdot [\![\boldsymbol{\phi}_{\top}]\!]_F + \nabla \cdot \boldsymbol{\phi}_{\top} [\![\alpha \boldsymbol{\phi} \cdot \mathbf{n}]\!]_F \right) \, dS.
\end{aligned}$$

Now  $B = 0$  is a direct consequence of the continuity conditions for  $\boldsymbol{\phi} \in \mathbf{X}(\Omega, \alpha) \cap \mathbf{PC}^{\infty}(\Omega, \mathcal{P})$ :

$$[\![\boldsymbol{\phi} \times \mathbf{n}]\!]_F = \mathbf{0} \text{ and } [\![\alpha \boldsymbol{\phi} \cdot \mathbf{n}]\!]_F = 0 \quad \forall F \subset \mathfrak{I}.$$

This completes the proof of the lemma.  $\square$

**Remark A.5.** Lemma A.4 is an extension to the Lemma 3.8 in [21] for Lipschitz polyhedron in the case when only homogeneous tangential boundary condition is satisfied for the vector field. It uses a similar argument to that of the Theorem 2.3 in [17]. In [17], no piecewise constant coefficients are involved, but the technique used shed light upon this kind of identity. The result in Lemma A.4 bears the same form with an identity valid for  $\mathbf{PH}^2(\Omega, \mathcal{P})$  regular vector fields used in Lemma 2.2 in [18]. In the proof of Lemma A.4, we further exploit the density result in [18], which implies this identity in [18] Lemma 2.2 holds for  $\mathbf{PH}^1(\Omega, \mathcal{P})$  regular vector fields when the jump conditions are met on the interfaces.

**Theorem A.6** (Weighted Helmholtz decomposition). *Under Assumption A.1, for any  $\mathbf{v} \in \mathbf{H}_0(\mathbf{curl}; \Omega)$ , there exist  $\psi \in H_0^1(\Omega)$  and  $\mathbf{w} \in \mathbf{PH}^1(\Omega, \mathcal{P}) \cap \mathbf{X}(\Omega, \beta)$  such that the decomposition (4.2) holds, and the estimate (4.3) is true.*

*Proof.* For any  $\mathbf{v} \in \mathbf{H}_0(\mathbf{curl}; \Omega)$ , let  $\psi \in H_0^1(\Omega)$  be the solution of

$$(\beta \nabla \psi, \nabla \phi) = (\beta \mathbf{v}, \nabla \phi), \quad \forall \phi \in H_0^1(\Omega).$$

It is easy to check that

$$\left\| \beta^{1/2} \nabla \psi \right\|_{\mathbf{L}^2(\Omega)} \leq \left\| \beta^{1/2} \mathbf{v} \right\|_{\mathbf{L}^2(\Omega)} \leq \|\mathbf{v}\| \quad (\text{A.6})$$

and that  $\mathbf{w} = \mathbf{v} - \nabla \psi$  satisfies

$$\nabla \cdot (\beta \mathbf{w}) = 0 \text{ in } \Omega \quad \text{and} \quad \mathbf{w} \times \mathbf{n} = \mathbf{0} \text{ on } \partial\Omega. \quad (\text{A.7})$$

The decomposition  $\mathbf{v} = \mathbf{w} + \nabla\psi$  shares the same form of the result (4.2) we want to prove, yet the rest is to show that  $\mathbf{w} \in PH^1(\Omega, \mathcal{P})$ . To this end, we first construct an  $\mathbf{H}^1$ -lifting of the  $\mathbf{w}$ . Using integration by parts we have

$$-\int_{\partial\Omega} \nabla\phi \cdot (\mathbf{w} \times \mathbf{n}) dS = \int_{\Omega} \nabla\phi \cdot \nabla \times \mathbf{w} = \int_{\partial\Omega} \phi \nabla \times \mathbf{w} \cdot \mathbf{n} dS \quad \forall \phi \in H^1(\Omega),$$

thus  $\mathbf{w} \times \mathbf{n} = \mathbf{0}$  on  $\partial\Omega$  implies  $\nabla \times \mathbf{w} \cdot \mathbf{n} = 0$  on  $\partial\Omega$  by a density argument (e.g. see [1]). Applying Theorem 3.17 in [1] on  $\nabla \times \mathbf{w}$ , there exists a  $\mathbf{w}_0 \in \mathbf{X}(\Omega, 1)$  such that

$$\begin{cases} \nabla \times \mathbf{w}_0 = \nabla \times \mathbf{w} & \text{in } \Omega, \\ \nabla \cdot \mathbf{w}_0 = 0 & \text{in } \Omega, \\ \mathbf{w}_0 \times \mathbf{n} = \mathbf{0} & \text{on } \partial\Omega. \end{cases}$$

Taking the convexity of the  $\Omega$  into account, an embedding result from Theorem 2.17 in [1] reads that  $\mathbf{X}(\Omega, 1) \hookrightarrow \mathbf{H}^1(\Omega)$ . Thus  $\mathbf{w}_0 \in \mathbf{H}^1(\Omega)$ . Obviously,

$$\nabla \times (\mathbf{w} - \mathbf{w}_0) = \mathbf{0} \text{ in } \Omega \quad \text{and} \quad (\mathbf{w} - \mathbf{w}_0) \times \mathbf{n} = \mathbf{0} \text{ on } \partial\Omega.$$

The simply-connectedness of  $\Omega$  implies that there exists a  $\zeta \in H^1(\Omega)$  (see Lemma A.2) with a constant boundary value such that

$$\mathbf{w} - \mathbf{w}_0 = \nabla\zeta \text{ in } \Omega.$$

By the fact that  $\mathbf{w}|_{\Omega_j}$  is divergence free within each  $\Omega_j$  respectively, and  $\llbracket \beta \mathbf{w} \cdot \mathbf{n} \rrbracket_F = 0$  for any  $F \subset \mathfrak{I}$ , one can check that the variational problem that  $\zeta$  satisfies is

$$(\beta \nabla\zeta, \nabla\phi) = - \sum_{F \subset \mathfrak{I}} \int_F \llbracket \beta \mathbf{w}_0 \cdot \mathbf{n} \rrbracket_F \phi dS \quad \forall \phi \in H_0^1(\Omega).$$

Noticing  $\llbracket \beta \mathbf{w}_0 \cdot \mathbf{n} \rrbracket_F = \llbracket \beta \rrbracket_F (\mathbf{w}_0 \cdot \mathbf{n})|_F \in H^{1/2}(F)$  on any  $F \subset \mathfrak{I}$ , the regularity result of Theorem 4.1 in [18] shows that  $\zeta \in PH^2(\Omega, \mathcal{P})$ , which is the piecewisely  $H^2$  smooth, while has  $H^1$  regularity across the interfaces. This, in turn, implies that

$$\mathbf{w} = \mathbf{w}_0 + \nabla\zeta \in PH^1(\Omega, \mathcal{P}) \cap \{\mathbf{v} \in \mathbf{X}(\Omega, \beta) : \nabla \cdot (\beta \mathbf{v}) = 0\}.$$

Lastly, to prove the estimate, by the triangle inequality and (A.6), we have

$$\|\beta^{1/2} \mathbf{w}\|_{\mathbf{L}^2(\Omega)} \leq \|\beta^{1/2} \mathbf{v}\|_{\mathbf{L}^2(\Omega)} + \|\beta^{1/2} \nabla\psi\|_{\mathbf{L}^2(\Omega)} \leq C \|\mathbf{v}\|.$$

It follows from Assumption A.1 (ii) and Lemma A.4 that

$$\sum_{j=1}^m \|\mu^{-1/2} \nabla \mathbf{w}\|_{\mathbf{L}^2(\Omega_j)} \leq C \sum_{j=1}^m \|\beta^{1/2} \nabla \mathbf{w}\|_{\mathbf{L}^2(\Omega_j)} = C \|\beta^{1/2} \nabla \times \mathbf{w}\|_{\mathbf{L}^2(\Omega)} \leq C \|\mathbf{v}\|.$$

These inequalities and (A.6) imply the validity of (4.3) and, hence, it completes the proof of the theorem.  $\square$

**Remark A.7.** *The decomposition result in Theorem A.6 resembles that of Theorem 3.5 in [18]: any vector field in  $\mathbf{X}(\Omega, \beta)$  can be split into a  $\mathbf{PH}^1(\Omega, \mathcal{P})$ -regular part, and a singular part solving a Dirichlet boundary problem  $-\nabla \cdot (\beta \nabla \psi) = f \in L^2(\Omega)$ . In the proof of Theorem A.6, we refine the results to cater the need for the pipeline of proving the reliability of the error estimator. Namely, when certain assumption of geometry is imposed, if a vector field  $\mathbf{v} \in \mathbf{X}(\Omega, \beta)$  and  $\nabla \cdot (\beta \mathbf{v}) = 0$ , the singular part is non-existent.*

## References

- [1] C. AMROUCHE, C. BERNARDI, M. DAUGE, AND V. GIRAUT, *Vector Potentials in Three-dimensional Non-smooth Domains*, Mathematical Methods in the Applied Sciences, 21-9(1998), pp. 823–864. **36**
- [2] C. A. BALANIS, *Advanced Engineering Electromagnetics*, John Wiley & Sons, Publishers, Inc., 1989. **34**
- [3] R. BECK, R. HIPTMAIR, R. W. HOPPE, AND B. WOHLMUTH, *Residual Based A Posteriori Error Estimators For Eddy Current Computation*, Math. Model. Numer. Anal., 34(2000), pp. 159–182. **2, 3, 4, 11, 12, 21, 22, 28**
- [4] C. BERNARDI AND R. VERFÜRTH, *Adaptive finite element methods for elliptic equations with non-smooth coefficient*, Numer. Math., 85-4(2000), pp. 579–608. **3, 12, 13, 14, 15, 18, 28**
- [5] D. BRAESS AND J. SCHÖBERL, *Equilibrated residual error estimator for edge elements*, Math. Comp., 77(2008), pp. 651–672. **2**
- [6] F. BREZZI AND M. FORTIN, *Mixed and Hybrid Finite Element Methods*, Springer, 1991. **8**
- [7] Z. CAI AND S. ZHANG, *Recovery-based error estimators for interface problems: conforming linear elements*, SIAM J. Numer. Anal., 47-3(2009), pp. 2132–2156. **3, 4, 21, 29**
- [8] Z. CAI AND S. ZHANG, *Recovery-based error estimators for interface problems: Mixed and nonconforming finite elements*, SIAM J. Numer. Anal., 48 (2010), pp. 30–52. **3, 29**
- [9] C. CARSTENSEN, *All First-Order Averaging Techniques for a Posteriori Finite Element Error Control on Unstructured Grids Are Efficient and Reliable*, Math. Comp., 73:247(2003), pp. 1153–1165.
- [10] C. CARSTENSEN AND R. VERFÜRTH, *Edge residuals dominate a posteriori error estimates for low order finite element methods*, SIAM J. Numer. Anal., 36(1999), pp. 1571–1587. **3, 19**

[11] L. CHEN, *iFEM: an innovative finite element methods package in MATLAB*, preprint, (2008). [27](#)

[12] J. CHEN, Y.XU, AND J.ZOU, *An adaptive edge element method and its convergence for a saddle-point problem from magnetostatics*, Numer. Methods PDEs, 28(2012), pp. 1643–1666. [2](#)

[13] J. CHEN, Y.XU, AND J.ZOU, *Convergence analysis of an adaptive edge element method for Maxwell's equations*, Appl. Numer. Math., 59(2009), pp. 2950–2969. [2](#)

[14] L. ZHONG AND S. SHU AND L. CHEN AND J. XU, *Convergence of adaptive edge finite element methods for  $H(\mathbf{curl})$ -elliptic problems*, Numerical Linear Algebra with Applications, 17(2010), pp. 415–432. [2](#)

[15] P.G. CIARLET, *The Finite Element Method for Elliptic Problems*, North-Holland, Amsterdam, 1978. [5](#)

[16] M. COSTABEL AND M. DAUGE, *Singularities of Electromagnetic Fields in Polyhedral Domains*, Arch. Rational Mech. Anal., 151-3(1997), pp. 221–276. [2](#)

[17] M. COSTABEL AND M. DAUGE, *Maxwell and Lamé Eigenvalues on Polyhedra*, Math. Meth. Appl. Sci., 22(1999), pp. 243–258 [3](#), [33](#), [35](#)

[18] M. COSTABEL, M. DAUGE, AND S. NICAISE, *Singularities of Maxwell interface problems*, Math. Model. Numer. Anal., 33(1998), pp. 627–649. [2](#), [3](#), [11](#), [33](#), [35](#), [36](#), [37](#)

[19] D., ROBERT AND LIONS, J.-L., *Mathematical Analysis and Numerical Methods for Science and Technology: Volume 3 Spectral Theory and Applications*, Springer, 2000. [1](#)

[20] P. FERNANDES AND G. GILARDI, *Magnetostatic and Electrostatic Problems in Inhomogeneous Anisotropic Media with Irregular Boundary and Mixed Boundary Conditions*, Mathematical Models and Methods in Applied Sciences, 7-7(1997), pp. 957–991. [11](#)

[21] V. GIRAUT AND P.-A. RAVIART, *Finite Element Methods for Navier-Stokes Equations: Theory and Algorithms*, Springer-Verlag, 1986. [33](#), [35](#)

[22] F. IZSÁK, D. HARUTYUNYAN, AND J. J. W. VAN DER VEGT, *Implicit a posteriori error estimates for the Maxwell equations*, Math. Comp., 77(2008), pp. 1355–1386. [2](#)

[23] R. HIPTMAIR, *Multigrid Method for Maxwell's Equations*, SIAM J. Numer. Anal., 36-1(1999), pp. 204–225. [1](#), [31](#)

[24] R. HIPTMAIR, J. LI, AND J. ZOU, *Convergence analysis of finite element methods for  $H(\mathbf{curl}; \Omega)$ -elliptic interface problems*, Numer. Math., 122-3(2012), pp. 557–578. [30](#)

[25] Q. HU, S. SHU, AND J. ZOU, *A discrete weighted Helmholtz decomposition and its application*, Numer. Math., 125(2013), pp. 153–189. [3](#)

[26] R. B. KELLOGG, *On the Poisson equation with intersecting interfaces*, Applicable Analysis: An International Journal, 4-2(1974), pp. 101–129. [29](#)

[27] P. MONK, *Finite Element Methods for Maxwell's Equations*, Oxford University Press, 2003. [2](#), [9](#), [12](#), [16](#), [18](#)

[28] J.-C. NÉDÉLEC, *Mixed finite elements in  $\mathbb{R}^3$* , Numer. Math., 35(1980), pp. 315–341. [2](#), [7](#)

[29] E. CREUSÉ AND S. NICAISE, *A posteriori error estimation for the heterogeneous Maxwell equations on isotropic and anisotropic meshes*, Calcolo, 40-4 (2003), pp. 249–271. [2](#)

[30] S. NICAISE, *On Zienkiewicz-Zhu error estimators for Maxwell's equations*, C. R. Acad. Sci., Paris, Sér. I, 340 (2005), pp. 697–702. [2](#), [28](#), [29](#)

[31] S. COCHEZ-DHONDT AND S. NICAISE, *Robust a posteriori error estimation for the Maxwell equations*, Comput. Methods Appl. Mech. Engrg., 196(2007), pp. 2583–2595. [2](#), [12](#)

[32] P.-O. PERSSON AND G. STRANG, *A simple mesh generator in MATLAB*, SIAM review, 46-2 (2004), pp. 329–345. [27](#)

[33] M. PETZOLDT, *A posteriori error estimators for elliptic equations with discontinuous coefficients*, Advances in Computational Mathematics, 16(2002), pp. 47–75. [3](#), [12](#), [13](#), [14](#), [15](#), [17](#), [18](#), [20](#), [28](#)

[34] J. SCHÖBERL, *A Posteriori Error Estimates for Maxwell Equations*, Math. Comp., 77(2008), pp. 633–649. [2](#), [12](#)

[35] P. ŠOLÍN, K. SEGETH, AND I. DOLEŽEL, *Higher-order Finite Element Methods*, CRC Press, 2004. [8](#)

[36] R. VERFÜRTH, *Error estimates for some quasi-interpolation operators*, Modél. Math. et Anal. Numér., 33(1999), pp. 695–713. [16](#)

[37] H. WHITNEY, *Geometric Integration Theory*, Princeton University Press, 1957. [8](#)

[38] J. XU, *Counterexamples concerning a weighted  $L^2$  projection*, Math. Comp., 57(1991), pp. 563–568. [14](#)

- [39] J. XU AND Z. ZHANG, *Analysis of recovery type a posteriori error estimators for mildly structured grids*, Math. Comp., 73-247(2004), pp. 1139–1152. 27
- [40] O. C. ZIENKIEWICZ AND J. ZHU, *A simple error estimator and adaptive procedure for practical engineering analysis*, International Journal for Numerical Methods in Engineering, 57(1987), pp. 337–357. 2
- [41] J. XU AND Y. ZHU, *Robust Preconditioner for  $H(\text{curl})$  Interface Problems.*, Domain Decomposition Methods in Science and Engineering XIX., 78(2011), pp. 173–180. 3